NASA Technical Memorandum 106905

Bulk Properties of $Ni_3Al(\gamma')$ With Cu and Au Additions

Guillermo Bozzolo
Analex Corporation
Brook Park, Ohio

and

John Ferrante
Lewis Research Center
Cleveland, Ohio

April 1995

National Aeronautics and
Space Administration

Bulk Properties of $Ni_3Al(\gamma')$ with Cu and Au additions

Guillermo Bozzolo[a] and John Ferrante[b]

[a] *Analex Corporation, 3001 Aerospace Parkway, Brook Park, OH 44142-1003, U.S.A.*

[b] *National Aeronautics and Space Administration, Lewis Research Center, Cleveland, OH 44135, U.S.A.*

Abstract

The BFS method for alloys is applied to the study of 200 alloys obtained from adding Cu and Au impurities to a Ni_3Al matrix. We analyze the trends in the bulk properties of these alloys (heat of formation, lattice parameter and bulk modulus) and detect specific alloy compositions for which these quantities have particular values. A detailed analysis of the atomic interactions that lead to the preferred ordering patterns is presented.

I. INTRODUCTION

The Ni_3Al (γ') phase in nickel-base superalloys is an unusual strengthening phase, very similar to the matrix in composition, with good oxidation resistance and with increasing yield strength with temperature [1]. Moreover, the inherent ductility of γ' prevents it from being a source of fracture, as opposed to the embrittlement generated by the formation of deleterious phases. Commercial nickel-base superalloys contain a number of alloying additions in order to modify specific properties of the superalloy (strength, creep resistance, etc.). These elements substitute and partition in γ' in different ways: Co substitutes for nickel, while Ti, Ta, Hf and Cb substitute for Al positions in the ordered structure. Mo, Cr and Fe substitute for both nickel and aluminum. Their effect in the mechanical properties is also varied: Hf improves the strength while Co, Mo or W retard the coarsening of γ'; increasing Cb markedly reduces the coarsening rate despite the concurrent increase in coherency strains; Mo raises the lattice parameter, solvus temperature and weight fraction of γ' in proportion to the Mo content of the γ'; etc. Several studies of commercial alloys have generated valuable experimental information on the mechanical and thermodynamical properties of these materials and their dependence on composition. However, it is only in the last few years that theoretical calculations at an atomic level have reached the point where the trends and behavior found experimentally can be compared with theoretical predictions. In spite of the theoretical and experimental body of work available, some basic issues related to the most essential features of these structures are still dubious: for example, different techniques provide conflicting results with regard to the site preference behavior of ternary additions [1]. Recent theoretical calculations have been geared to shed some light on these issues providing much needed insight on the electronic structure and the behavior of these systems [1].

In this work we take the first step in a line of research that will complement basic electronic structure calculations as well as the existing body of experimental data, by developing a semiempirical approach to the study of nickel-base superalloys. We will apply the semiem-

pirical BFS method for alloys [2–11] to the study of the Ni_3Al alloy and the effect of metallic impurities (Cu, Au) in the bulk properties of the alloy (lattice parameter, bulk modulus and heat of formation) while at the same time drawing conclusions on site preference of the ternary additions as well as the effect of ordering on the stability of these structures. Our main goal is to determine trends - which can be easily be confirmed experimentally - and to determine the potential of this type of approach for the analysis of complex macroscopic materials. We have performed extensive analysis of 200 ordered structures (binary, ternary and quaternary) and computed the bulk properties of these alloys as a function of composition. In doing so, we intend to shed some light on some of the basic questions discussed above (i.e., site preference) as well as to gain a better understanding of the interplay between the additions and the base elements and how that affects the basic properties of the alloy.

The BFS method for alloys [2,11] has been very successful in a variety of problems, ranging from the study of segregation profiles in binary alloys [5] to the theoretical modelling of tip-substrate interactions in an atomic force microscope [6]. More recently, BFS was successfully applied to describe the novel phenomenon of surface alloy formation of immiscible metals [10]. Based on the record of past performance of BFS, we restrict our present calculation to a limited number of ternary additions, for which the BFS parameters needed (see Ref. [8]) have been tested and proven in previous applications. A parallel effort to the present one, to be published elsewhere, deals with the challenge of extending the number of systems amenable to study with a similar degree of reliability. The four elements for which BFS parameters are needed are Ni, Cu, Al and Au: they have been previously used in applications to surface segregation (Ni/Cu, Ni/Au, Cu/Au) [5], surface alloy formation (Ni/Au) [10], multilayer relaxation and surface structure of ordered alloys (Cu/Au, Ni/Al) [7,11] and composition dependence of bulk properties of ordered binary alloys (Ni/Al, Cu/Ni, Al/Au, Cu/Au) [9].

In terms of experimental data to compare with our results, there is not much documented for the ordered ternary and quaternary ordered structures. While abundant data exists for the binary alloys (Al-Au, Al-Cu, Al-Ni, Au-Cu, Au-Ni, Cu-Ni) to our knowledge no quater-

nary alloys and only a few ternary structures have been studied. The crystal structure and lattice parameters are known for AuCuNi, $Au_7Cu_{10}Ni$, $Au_9Cu_{10}Ni$, Al_2Cu_2Ni, $Al_2Cu_3Ni_{15}$, $Al_{15}Cu_{24}Ni$ and $Al_{31}Cu_{16}Ni_4$ [13].

We organize the paper as follows: in Section 2 we briefly describe the BFS method, in Section 3 we present fully-relaxed BFS results obtained for the heat of formation, lattice parameter and bulk modulus as a function of composition for a large number of binary, ternary and quaternary alloys obtained by adding Cu and Au atoms to a γ' Ni_3Al phase. Concluding remarks are included in Section 4.

II. THE BFS METHOD

Since its inception two years ago, the BFS method has been applied to a variety of problems [2–11], starting with the basic analysis of bulk properties of solid solutions of fcc and bcc binary alloys (heat of formation [2,3], lattice parameter [4], etc.) and more specific applications like the energetics of bimetallic tip-sample interactions in an atomic force microscope [6] as well as Monte Carlo simulations of the temperature dependence of surface segregation profiles in Cu-Ni alloys [5]. Other applications include surface structure of metallic alloys [7,11] and a diagramatic analysis of ordered alloy clusters for the determination of the ground state structure of a given binary alloy [12]. An additional advantage of BFS is that it allows for deriving simple, approximate expressions which describe the trends in segregation as well as elucidating the driving mechanisms for these phenomena. Also, as a consequence of the ideas underlying the foundation of BFS, simple expressions for predicting the composition dependence of bulk alloy properties based solely on pure component properties have been recently derived, providing an alternative to the commonly used Vegard's law [9].

In what follows we present a brief review of the method. Due to its novel way of partitioning the energy in different contributions, this presentation should be complemented with a review of previous applications (see Ref. [11], in order to familiarize the reader with the main concepts discussed below.

The BFS method is based on the idea that the energy of formation of an arbitrary alloy structure is the superposition of individual contributions ε_i of nonequivalent atoms in the alloy,

$$\varepsilon_i = \varepsilon_i^S + g_i(\varepsilon_i^C - \varepsilon_i^{C_0}). \tag{1}$$

so that the total energy of formation is

$$\Delta H = \sum_i \varepsilon_i \tag{2}$$

For each atom, we break up the energy into two parts: a strain energy ε^S and a chemical contribution, linked by a coupling factor g:

$$\epsilon_i = \epsilon_i^{strain} + g_i \epsilon_i^{chem} \tag{3}$$

where i denotes the atomic species of a given atom (ϵ_0^C is a reference energy to be defined later).

The strain energy, ϵ_i^S, accounts for the actual geometrical distribution of the atoms surrounding atom i, computed as if all its neighbors were of the *same* atomic species as atom i. ϵ_i^S is then evaluated with any available technique.

The coupling term, g_i, is related to the strain energy in the sense that it contains information on the structural defect included in ϵ_i^S. In order to establish this connection, based on the assumption that the universal binding energy relationship of Rose et al. [14] contains all the relevant information concerning a given single-component system, we write

$$\epsilon_i^S = E_C^i F^*(a_i^{S*}) \tag{4}$$

where

$$F^*(a^*) = 1 - (1 + a^*)e^{-a^*}, \tag{5}$$

and where a_i^{S*},given by

$$a_i^{S*} = q\frac{(a_i^S - a_e^i)}{l_i}, \tag{6}$$

is a scaled lattice parameter related to a_i^S, a quantity that contains the structural information of the defect crystal. a_e^i ,l_i and E_C^i, are the equilibrium lattice parameter, scaling length and cohesive energy of a pure crystal of species i and $q^3 = \frac{3}{16\pi}$ for fcc metals.

Once ϵ_i^S is evaluated by any theoretical means, a_i^{S*} can be easily obtained from Eq.(4) with which the coupling term g_i becomes

$$g_i = e^{-a_i^{S*}}. \tag{7}$$

As in previous efforts, we choose equivalent crystal theory (ECT) [15,16] to perform strain energy calculations, the choice being guided by the simplicity and reliability of this technique. Using ECT for computing ϵ_i^S introduces the added advantage that a_i^S (and thus

a_i^{S*}) is directly obtained by solving the ECT equation for the defect crystal, as shown below. Within the framework of ECT [15], a_i^S is interpreted as the lattice parameter of an ideal, perfect crystal (i.e., the equivalent crystal) where the energy per atom is the same as the energy of atom i in the actual, defect crystal.

In general, the ECT equation for computing the strain energy reads

$$NR_1^p e^{-\alpha R_1} + MR_2^p e^{-(\alpha+\frac{1}{\lambda})R_2} = \sum_j r_j^p e^{-(\alpha+S(r_j))r_j} \tag{8}$$

(see Ref. [16] for details) where the quantities p, α, λ and the screening function S are defined in Refs. [15,16]. The sum on the r.h.s. of Eq. (8) runs over all neighbors of atom i at a distance r_j. Eq. (8) is then solved for the lattice parameter of the equivalent crystal a_i^S. R_1 and R_2 are the corresponding nearest- and next-nearest-neighbor distances in the equivalent crystal. The strain energy is then computed with Eq.(4). For the particular case where all the neighboring atoms are located at lattice sites, $r_j = r_1$ and $S(r_1) = 0$ for nearest-neighbors, $r_j = r_2$ and $S(r_2) = 1/\lambda$ for next-nearest-neighbors and, if n is the actual number of nearest-neighbors and m is the corresponding number of next-nearest-neighbors, then eq. (8) is simply

$$NR_1^p e^{-\alpha R_1} + MR_2^p e^{-(\alpha+\frac{1}{\lambda})R_2} = nr_1^p e^{-\alpha r_1} + mr_2^p e^{-(\alpha+\frac{1}{\lambda})r_2}. \tag{9}$$

Rigourously, the computation of the strain energy includes four terms (see Ref. [15]). In this work, we neglect the three- and four-body terms dealing with the bond angle and face-diagonal anisotropies and retain only the two-body term that accounts for bond-length anisotropies [15], which we expect to be relevant for atoms in the top (surface) layers. The higher order terms would be proportional to the small local fluctuations of the atomic positions around the equilibrium lattice sites. We expect that the leading term, Eq. (4), will adequately account for these small distortions.

The chemical contribution ε_i^C is obtained by an ECT-like calculation. As opposed to the strain energy term, the surrounding atoms *retain their chemical identity*, but are forced to be in equilibrium lattice sites. If N_{ik} (M_{ik}) denotes the number of nearest(next)-neighbors

of species k of the atom in question (of species i) then the ECT equation [15,16] to be solved for the equivalent lattice parameter a_i^C is

$$NR_1^{p_i}e^{-\alpha_i R_1} + MR_2^{p_i}e^{-(\alpha_i+\frac{1}{\lambda_i})R_2} = \sum_k N_{ik}r_1^{p_i}e^{-\alpha_{ik}r_1} + \sum_k M_{ik}r_2^{p_i}e^{-(\alpha_{ik}+\frac{1}{\lambda_i})r_2} \tag{10}$$

where $N(M)$ is the number of nearest(next)-neighbors in the equivalent crystal of species i and $R_1(R_2)$ is the nearest(next)-neighbor distance in the equivalent crystal of lattice parameter a_i^C. r_1 and r_2, are the equilibrium nearest- and next-nearest-neighbor distances in an equilibrium crystal of species i, respectively. The chemical energy is then computed with

$$\varepsilon_i^C = \gamma E_C^i F^*(a_i^{C*}) \tag{11}$$

and

$$\varepsilon_{0_i}^C = \gamma_0 E_C^i F^*(a_{0_i}^{C*}) \tag{12}$$

where $\gamma(\gamma_0) = +1$ if $a_i^{C*}(a_{0_i}^{C*}) \geq 0$ and $\gamma(\gamma_0) = -1$ otherwise, and $a_i^{C*} = q(a_i^C - a_e^i)/l_i$. The scaled lattice parameter a_i^{C*} is obtained from Eq.(10) with the parameters α_{ik} listed in Ref. [8], and $a_{0_i}^{C*}$ is computed by solving Eq.(10) but with $\alpha_{ik} = \alpha_i$. The rest of the parameters appearing in Eq.(10) are listed in Ref. [15].

Even though BFS is a semiempirical method, its dependence on experimental input is minimal in that *only* two experimental (or theoretical) alloy values (in the present study the heats of solution in the dilute limit were used [17]) are needed. The remaining input are pure element properties, the cohesive energy, equilibrium bulk modulus and lattice parameters. In this work, we used the parameters Δ_{AB} and Δ_{BA} determined following the procedure outlined in Ref. [2] . The experimental input, as well as the resulting BFS parameters can also be found in Ref. [8]. The ECT and BFS parameters used in this work for Ni, Al, Cu and Au are listed in Tables 1 (ECT) and 2 (BFS).

We should emphasize that in the context of BFS, the strain and chemical energy contributions differ substantially in meaning from the one these terms have in other approaches. The BFS strain energy is related to the usual strain only in that the atomic locations are

those found in the actual alloy: the BFS strain energy of a given atom is then the actual strain that it would have in a monatomic crystal of the same species of the reference atom. Likewise, the BFS chemical contribution is related to the usual chemical energy in that the actual chemical composition of the alloy is taken into account, but with the neighboring atoms located in ideal atomic sites: the BFS chemical energy of a given atom is then the actual chemical energy in an ordered environment with the lattice spacing characteristic of the equilibrium lattice of the reference atom. Therefore, the BFS contributions are, in a sense, a certain combination of the actual strain and chemical energies. We refer the reader to previous applications of BFS for more insight in this issue.

In this work, we focus our attention on four elements, namely Ni, Al, Cu and Au, for which the BFS parameters are well-known and have been used in previous applications. However, in order to ensure a good description of the energetics of the basic system (Ni_3Al), we used a different set of values for Δ_{NiAl} and Δ_{AlNi}, determined by fitting to equilibrium properties, i.e. heat of formation (-0.3914 eV/atom) and lattice parameter (3.563 Å), of the Ni_3Al alloy. Fortunately, the BFS parameters obtained in this fashion do not differ much from the ones previously determined by fitting to the theoretical estimates of the heat of solution in the dilute limit computed by Carlsson and Sanchez [18] in their simulation of Ni-Al alloys. This fact gives us confidence on the reliability of the parameters used in this calculation . It is to be expected then that the bulk properties of the basic Ni_3Al alloy will be properly reproduced by BFS, as well as small departures from this ground state structure after Ni or Al enrichment or after the introduction of impurities. Both sets of parameters are listed in Table 1.

III. RESULTS AND DISCUSSION

The main purpose of this paper is to investigate trends in the behavior of the bulk properties of nickel-base superalloys after the introduction of specific metallic impurities. There is no *a priori* criterion that can be used to determine which configurations will be preferred, as it is precisely our concern to examine intituively unlikely configurations that can be found to be favorable due to the unexpected interaction between the different atomic species and the influence, for fixed compositions, of the relative locations of these atoms. In what might appear as a brute force approach, it serves then our purposes to consider a sufficiently large number of seemingly arbitrary choices for atomic distributions and determine from them different patterns of behavior. From an initially large number of configurations studied, we retained those that are unique in that no symmetry operation makes any listed configuration redundant. This set includes 200 ordered structures which can be divided into four separate groups: i) configurations # 1 through # 44, which correspond to Ni-Al alloys where the Ni concentration varies from 66.7 to 83.3 at. % Ni, which comfortably covers the range of Ni concentration for which a Ni_3Al phase with the Cu_3Au ($L1_2$) structure is found in the phase diagram. ii) configurations # 45 through # 100 corresponding to ternary Ni-Al-Cu alloys, iii) configurations # 101 through # 156, a replica of the previous set but for Ni-Al-Au alloys and iv) configurations # 157 through # 200, which includes a small set of interesting quaternary ordered structures of Ni, Al, Cu and Au. As it will be seen below, this set of configurations proves to be large enough not only to understand the general trends in the bulk properties of the corresponding alloys, but also to help us determine 'missing' configurations, based on regularities found in the concentration dependence of the bulk properties. Moreover, the simplicity of the BFS scheme helps us to understand what are the essential ingredients governing the behavior found in these systems.

To provide a detailed description of all 200 configurations using the standard notation would be long and tedious and, moreover, it would not facilitate a quick visualization of the different configurations considered, some which have very low symmetry. We therefore

developed a simpler and concise way of describing the sample set which overcomes this difficulty as it relies on a straightforward labeling algorithm and notation. All changes in atomic location and substitution of different atomic species were performed in a cell consisting of 48 atoms. Fig. 1.a shows a portion of this cell for the ground state Ni_3Al case, with the Ni and Al atoms located following the $L1_2$ distribution. These atoms are then labeled following the pattern indicated in Fig. 1.b. The cell in Fig. 1.a follows the stacking sequence ABCD. Each atom is identified by the plane to which it belongs and the numebring sequence within each plane indicated in Fig. 1.b. In what follows any change in identity or location is referred to by the label as indicated in Fig. 1. The ground state structure contains 36 Ni atoms and 12 Al atoms. Changes in chemical composition will be therefore indicated with the symbol $A_n \rightarrow B_n$, i.e. an atom of species A in the site n is substituted by an atom of species B. An exchange in location of a given pair of atoms is indicated by $A_n \leftrightarrow B_m$, indicating that an atom A in site n trades places with an atom B in site m. When more than one pair of atoms are exchanged, site labels are listed in an orderly fashion. For example, $A_{nm} \leftrightarrow B_{kl}$ stands for two exchanges: $A_n \leftrightarrow B_k$ and $A_m \leftrightarrow B_l$. Once again, the Ni_3Al structure shown in Fig. 1 is used as the reference state. Only for the purpose of this paper, we find it more convenient to introduce the label $(n_{Al},m_{Ni},k_{Cu},l_{Au})$ to indicate the composition of the alloy. Keeping in mind that the ground state has 36 Ni atoms and 12 Al atoms in the primitive cell, the indices n and m denote the number of extra (if positive) or substituted (if negative) Al and Ni atoms respectively, whereas k and l denote the number of Cu and Au impurities present. Then, the ground state is denoted with (0,0,0,0) and an alloy like $Ni_{0.5}Al_{0.25}Cu_{0.125}Au_{0.125}$ is simply indicated with the symbol (0,-12,6,6), which means that all 6 Cu atoms as well as the 6 Au atoms occupy Ni sites. A pure Ni crystal is then (-12,12,0,0) and a pure Al crystal is (36,-36,0,0). We will keep $n + m + k + l = 0$, which means that no vacancies are considered in this calculation. In Appendix 1 we list the transformations needed to construct the 200 alloys considered following the notation introduced in this section. Also, Fig. 2 shows some configurations which will be of interest later.

A. Ni-Al alloys

We will analyze the results of this calculation with respect to the four groups of alloys indicated above. We will first deal with pure Ni-Al compounds. Obviously, the 'ground state' (0,0,0,0) belongs to this group. We have studied alloys that depart from stoichiometric Ni_3Al for the range of concentrations 67-83 at.% Ni, which includes such ordered structures as Ni_2Al and Ni_5Al. This set therefore includes structures that range from (4,-4,0,0) to (-4,4,0,0). For each composition (m,n,0,0) we considered a few variations by having some Ni and Al atoms exchange positions. Not surprisingly, there is a definite increase in heat of formation with increasing disorder, i.e. increasing number of Ni $\leftrightarrow$ Al exchanges. Fig. 3 displays the heat of formation of all the (Al,Ni,0,0) structures studied as a function of composition: as expected, there is a clear V-shaped boundary line with the vertex at the ground state Ni_3Al structure. The configurations that lie on this line are characterized by simple substitutional Ni or Al additions, with no exchanges. Also, as expected, the slope of the Ni-rich branch of this line is greater than that of the Al-rich side. Obviously, the controling factor in deciding the location of a given structure in Fig. 3 is dictated by the relative position of the substitutional atoms: for example, while configurations # 37 and # 38 are essentially similar, the only difference resides in the fact that the substitutional atoms are nearest-neighbors of each other (# 37) or next-nearest-neighbors (# 38). Therefore, in # 38 the number of Al-Ni bonds is maximized with respect to # 37 where it is minimized. This reflects in Fig. 3 where # 37 and # 38 are at opposite ends of the spectrum for that composition. For clarity, these two configurations as well as others that will be of interest later are displayed in Fig. 2.

If the number of Ni-Al bonds is the essential ingredient for stabilizing the structure, then this also explains why Al-rich alloys are more stable than Ni-rich ones: in the Al-rich alloys, Al atoms occupy Ni sites, thus creating 4 Al-Al bonds and 8 Ni-Al ones. In a Ni-rich alloy, the Ni atom in an Al site creates 12 Ni-Ni bonds, increasing the strain and the chemical energy, in addition to the loss of several Ni-Al favorable bonds. With the term 'favorable'

we mean that, within the context of BFS, those bonds give a negative contribution to the BFS chemical energy thus lowering the heat of formation.

The lattice parameter dependence on composition, shown in Fig. 4, shows similar features, except for the fact that Ni-rich alloys are smaller, as it is to be expected due to the smaller size of Ni atoms. Moreover, the rate of decrease of the lattice parameter as Ni atoms are added is much smaller than the rate of increase when Al atoms are added. An indication of how a more realistic simulation could be carried out, is given by well known features of another Ni-Al alloy: the NiAl phase which has the ordered CsCl (B2) structure. It is known that the lattice parameter decreases for *both* the Ni-rich and Al-rich regimes. The decrease in the Ni-rich side is due to $Al \rightarrow Ni$ substitutions, but the decrease on the Al-rich side is due to the presence of vacancies in the Ni sites. Otherwise, one would expect the lattice parameter to increase in that region due to the size difference between Al and Ni atoms. Therefore it is to be expected that more stable states than the ones presented here should be found if vacancies were allowed to exist, which, as noted before, have not been included in this work.

In Fig. 3, configurations with the lowest heat of formation can be joined by a straight line. A similar behavior is found for the lattice parameter: configurations with the smallest value of a for each composition lie on a straight line. This, together with the fact that there is a perfect correspondence between the ordering of the spectrum (for each composition) of the configurations in Fig. 4 with those in Fig. 3, gives us a criterion to determine the size and structure of other stable structures. For example, there is evidence that an ordered structure exists for (6,-6,0,0) (Ni_5Al_3). Although it is not an fcc-based alloy (it has a Ga_3Pt_5 (oC16) structure), our calculations predict a lattice parameter of 3.6252 Åand a substantially lower heat of formation than the one that would be obtained by extrapolating on the V-shaped boundary line in Fig. 3: -0.2997 eV/atom vs. an extrapolated value of -0.28 eV/atom. These results give credibility to the slight curvature seen at the extremes of the boundary line (see configurations # 36, 38, 43 and 44), which could be taken as an indication for the existence of other stable ordered structures at other compositions (i.e., while (0,0,0,0) is the

ground state for 3:1 composition, the boundary line would attain a local minimum value at 5:3, much higher in energy than (0,0,0,0) probably due to the fact that the ordered alloy considered in this work is forced to have the same lattice type as Ni_3Al).

Fig. 5 displays the values of the bulk modulus B for the configurations shown in figs. 2 and 4. Once again, a boundary line is clearly defined with two different regimes for Ni- or Al-rich alloys: not surprisingly, there is a noticeable decrease in the value of B for Al-rich alloys while there is a less steep increase in its value for Ni-rich alloys. The fact that the alternative structures (i.e., those that include Ni $\leftrightarrow$ Al exchanges) lie below the boundary line indicate that in every case, whether there is Ni or Al abundance, the net effect of site exchanges is always that of lowering the value of B.

To conclude the presentation of (Al,Ni,0,0) results, Fig. 6 displays the change in heat of formation from the rigid (i.e., the Ni_3Al structure) to the relaxed value (from which the lattice parameters and bulk moduli in the previous figures were obtained). Two distinct regimes can be seen in this figure: for Ni-rich alloys there is almost no change in the heat of formation as compared to the change seen for Al-rich alloys. This behavior results from the competition between the BFS strain and chemical energy contributions described above. It is also useful to define the effective coordination of a given atom in order to understand this behavior [10]. The calculation of the BFS strain energy (to a nearest-neighbor approximation) is based on a 'measure' of the defect as seen by a given atom. Eq. (9) establishes a relationship between the defect crystal (r.h.s. of the equation) and the equivalent crystal (l.h.s.). The term to the left could be understood as a measure of the defect, given by (in a nearest-neighbor approximation) $q_d = nr^p e^{-\alpha r}$, where n is the number of nearest-neighbors located at a distance r of the atom in question (assuming, as is the case in this calculation, that the separation distance is the same in all cases). The parameters p and α depend on the species of the reference atom [11,16]. Equilibrium (a situation for which both sides of eq. (8) are identical) correspond to $q_e = Nr_e^p e^{-\alpha r_e}$, where $N = 12$ and $r_e = \sqrt{2}a_e/2$ (for fcc metals). Although every atom in these alloys has ideal coordination (N=12), we should account for the fact that they find themselves in chemically mixed environments as well as

different in size with respect to their equilibrium state. We therefore ask ourselves what is the effective number of Ni nearest-neighbors that will simulate the equilibrium situation for that same Ni atom in the Ni_3Al (i.e., what is the value of n for which $q_d = q_e$):

$$n r_X^{p_{Ni}} e^{-\alpha_{Ni} r_X} = N r_{Ni}^{p_{Ni}} e^{-\alpha_{Ni} r_{Ni}} \tag{13}$$

where r_X is the equilibrium nearest-neighbor separation distance in the Ni_3Al and r_{Ni} the corresponding length in a ground state Ni crystal. Using the parameters in Table 1, a Ni atom in an equilibrium Ni_3Al lattice has, in BFS terms, an effective coordination of 11.8 atoms while an Al atom in the same lattice has an effective coordination of 15 atoms. This concept quantifies the obvious fact of the size difference between Ni and Al atoms. One would then expect BFS strain effects to guide the relaxation of Al-rich alloys, therefore introducing large gains in energy with respect to the equilibrium Ni_3Al configuration. At the same time, this effect is modulated by the creation of Ni-Al bonds discussed above, which are responsible for the stability of the structure. Altogether, these arguments suggest that further gain can be achieved by the creation of vacancies in Ni sites which is precisely what is experimentally found. On the other side (Ni-rich alloys), substitution of Al atoms with Ni atoms greatly reduces the BFS strain but also lowers the chemical effect of Ni-Al bonds. The competition of these two effects result in small net changes in the heat of formation with respect to the rigid Ni_3Al equilibrium structure.

The numerical results corresponding to Figs. 3, 4 and 5, together with the values for the cohesive energy, are listed in Table 3.

B. Al-Ni-Cu alloys

The second group includes ternary Ni-Al-Cu alloys, with Cu concentrations ranging from 0 to 19 at.% Cu. The results for the heat of formation of the $L1_2$ ordered structures are displayed in Fig. 7 as a function of Ni concentration. Being that the impurity atoms can occupy Ni as well as Al sites, we introduce different symbols to indicate different (m,n,k,0)

states: for example, □86[5] indicates configuration # 86 with 9 Cu atoms (□) with 5 of them occupying Al sites and ∗73[2] denotes configuration # 73 with 3 Cu atoms (∗) with two of them in Al sites. For the sake of clarity, we include these configurations in Fig. 2. Once again, none of the configurations studied has a lower heat of formation than the one corresponding to Ni_3Al, as was the case for (Al,Ni) alloys. Also, a boundary line can be defined with the whole spectrum contained above this line. The fact that all the configurations belonging to the boundary line are of the type [0] (i.e. no Cu atoms in Al sites) indicates that the most stable alloys correspond to those where the Cu atoms occupy only Ni sites. The few configurations of the type (0,-b,b,0) that do not lie on this line (for example, # 70, # 63, etc.) correspond to those where in addition to the substitution of Cu atoms we also considered exchange of Ni and Al atoms, which as seen previously for (Al,Ni) alloys always results in an increase in energy. A pattern emerges when looking at the structure of the configurations belonging to the boundary line: the impurity atoms tend to occupy Ni sites on the same plane, so that the stacking is of the type ABABA.. where A denotes a 1:1 Ni:Al plane and B denotes a plane with varying numbers of Cu and Ni atoms. The heat of formation will be lower the smaller the number of Cu-Ni bonds. That is clearly seen in configuration # 100 (shown in Fig. 2), where the Cu atoms occupy Al sites thus maximizing the number of unfavorable Cu-Ni bonds. Fig. 8 displays the configurations (# 58, 65, 82, 87, 90 and 99) belonging to this boundary line.

Fig. 9 shows results for the lattice parameter of ternary Al-Ni-Cu alloys: two different regimes to the left and right of the ground state are seen. Cu and Ni have similar sizes, therefore, one would expect few changes in the lattice parameter for those alloys where Cu occupy Ni sites. That is not the case: there is a noticeable increase in lattice parameter with increasing number of Cu impurities in Ni sites. This is clearly due to the increasing number of unfavorable Cu-Ni bonds, thus inducing relaxation of the system in a trade-off between the ensuing increase in BFS strain energy and decrease in BFS chemical repulsion. This also explains the fact that configurations that are higher in energy (for example, # 95 shown in Fig. 2) have a much smaller lattice parameter: in # 95, the six Cu atoms occupy

two Al sites and four Ni sites therefore increasing the number of chemically favorable Cu-Al and Ni-Al bonds and consequently reducing the need for relaxation. In general, the lattice parameter decreases as the Cu atoms locate themselves in Al sites. This analysis indicates that some configurations are 'missing' if one wanted to define a boundary line in Fig. 9 joining those states with the smallest values for the lattice parameter for each concentration which are not, clearly, those shown to the far left in Fig. 9.

The values for the bulk modulus are displayed in Fig. 10: as it was mentioned in the previous paragraph, those same 'missing' configurations would constitute the boundary line in Fig. 10 with maximum values of B. As expected, substitution of Ni atoms by Cu atoms substantially lowers the value of B.

We conclude the analysis of Al-Ni-Cu alloys by commenting on the relaxation energies with respect to the equilibrium ground state (0,0,0,0) which, as expected, represent a small percentage of the rigid heat of formation, as indicated in Fig. 11. The largest percentage change corresponds to •49[0], where the Cu atom occupies a Ni site and four Ni $\leftrightarrow$ Al exchange occur, so that the number of Cu-Al bonds is maximized at the expense of Ni-Al bonds. Numerical values for the bulk properties of the alloys discussed in this section are listed in Table 4.

C. Al-Ni-Au alloys

For the same range of Cu concentration studied in the previous paragraph, we now consider the effect of introducing Au atoms. Quite a different behavior is seen for Al-Ni-Au alloys, although we once again have a situation where two of the possible binary alloys exist (Al-Au and Al-Ni), and one (Ni-Au) does not. It is then somewhat surprising that, given this similarity with the Al-Ni-Cu case, it is found that several configurations yield lower values for the heat of formation than the one found for the ground state Ni_3Al, as shown in Fig. 12. These configurations (# 135, # 150, etc.) share the fact that the Au atoms occupy Ni sites, which is surprising in the sense that one would expect Au atoms to replace atoms of similar

size (Al) in order to keep the BFS strain low. Substitutions of the type $Ni \leftarrow Au$ significantly reduce the number of unfavorable Ni-Au bonds. Chemical energy effects therefore dominate the behavior of these alloys strongly favoring those structures where the Au atoms locate themselves in Ni sites generating structures with stacking ABCB..., where A is a pure Ni plane, B is a 1:1 Ni:Al plane and C is a 1:1 Au:Ni plane. One would then expect further gains by introducing more Au atoms so that C is a pure Au plane. That is not the case: by doing so, the BFS strain energy for Au atoms becomes the dominant factor, far outweighting the gains realized by the chemically favorable bonds thus created. That can be seen in configuration # 155, where plane C has 3:1 Au:Ni composition but much higher heat of formation than # 150. Actually, configuration # 150 is in this sense ideal, as the Au atoms alternate with Ni atoms thus maximizing the number of chemically favorable bonds. Configurations # 150 and 155 are included in Fig. 2.

The values for the lattice parameter for these alloys is displayed in Fig. 13. As was the case for Al-Ni-Cu alloys, Au atoms induce relaxations that are larger when they occupy Al sites instead of Ni sites, as a result of the competition between the strain and chemical contributions to the energy. The relaxations are much larger than in the Al-Ni-Cu case. The contractions are not as noticeable. Another difference resides in the fact that while in the Al-Ni-Cu case the substitution of Al atoms by Cu induced contractions, substitution of Al atoms by Au atoms induce expansions (see configurations # 100 and # 156 as examples of this), once again, as a result of the competition between strain and chemical effects.

The values of the bulk modulus are displayed in Fig. 14, showing a decrease when Au atoms occupy Ni sites and a less markedly increase when they occupy Al sites. Finally, Fig. 15 shows the change in energy between the relaxed and the rigid $L1_2$ structures, which represent a direct consequence of the large relaxations shown in Fig. 13. Numerical results for all the (n,m,0,h) alloys are listed in Table 5.

D. Al-Ni-Cu-Au alloys

The two different behaviors found for Cu or Au ternary additions, and the trends observed in the dependence of their bulk properties on composition suggest that quaternary alloys (Al,Ni,Cu,Au) could exhibit interesting properties as a consequence of the different ingredients that enter in competition. The analysis of Al-Ni-Cu alloys indicated a tendency towards the formation of stable structures when Cu atoms occupy Ni sites with alternating Ni-Al and Cu-Ni planes. Also, we discussed the finding of a ternary Al-Ni-Au alloy (configuration # 150) with an apparently optimum balance of BFS strain and chemical contributions to provide a very low value for the heat of formation. It was also seen that increasing Au concentration (leading, for example, to configuration # 155) was enough to break that balance: the BFS strain increased with no compensatory creation of favorable bonds. This situation could then be improved if a fourth element is introduced without changing the strain energy much, but creating a larger number of favorable bonds. This is achieved, for example, by introducing Au atoms. The stabilizing effect of introducing Au impurities in the Al-Ni-Cu alloys is seen in Fig. 16, which shows the values of the heat of formation for some quaternary alloys (n,m,k,h). The best example is given by configuration # 168, with composition (0,-6,3,6), where all three Cu atoms, as well as the six Au atoms occupy Ni sites in the same plane in an alternate fashion, thus maximizing the number of Cu-Au bonds which favorably contribute to the chemical energy of the alloy. The structure has stacking ABCB..., where A is a pure Ni plane, B a 1:1 Ni:Al plane and C is 3:3:6 Ni:Cu:Au. Further extensions of this ordering could only favor the stability of the system by maximizing the effect. One would therefore expect ordered structures with an extension of these patterns to have substantially lower values of ΔH. Configurations # 169 and # 171 amplify the gain by duplicating the mixed Au-Cu-Ni plane, achieving the lowest values for the heat of formation for the whole set of configurations, whereas # 172, while very low in energy, slightly breaks the delicate balance with the additional introduction of Cu atoms. The lattice parameter of these alloys attain intermediate values between the ones obtain for

the two type of ternary alloys studied in previous sections, as is also the case for the bulk modulus. However, configurations # 168, # 169 and # 171 (shown in Fig. 2, together with # 172) distinguish themselves from the rest not only by their low heats of formation but also by their high value of B, which when compared to characteristic values of B for Al-Ni-Cu alloys, seem to ignore the presence of the the Cu atoms reaching values in the range that corresponds to Al-Ni-Au compounds.

While this group of alloys (represented basically by # 169-171) distinguis themselves because of their low values of ΔH, a different group of alloys stands out because of the large values achieved for the bulk modulus. Configurations # 183-190 are characterized by values of ΔH similar to those of Ni_3Al, and values for the lattice parameter comparable to the previous group (# 169), but the typical values of the bulk modulus B of these alloys is much higher than any of the other alloys studied in this work. For example, the composition of configuration # 190 is (-6, -12, 6, 12), the only difference with respect to # 169 of composition (0,-18,6,12), being the Ni and Al concentrations, based on a different distribution of the subsitutional impurities. Moreover, close examination of configurations # 189 and # 190 indicates that little change occurs in the bulk properties of these alloys when Al atoms 'segregate' to a separate plane. This hints to the possibility that stable phases of ternary alloys of Ni, Cu and Au might exist.

Figs. 17 and 18 show the values for the lattice parameter a and bulk modulus B for these alloys. Numerical results for the bulk properties of these alloys are listed in Table 6.

The results presented in this work can be best summarized by showing the complete set of configurations in one single figure for each bulk property, therefore allowing for comparison of the trends for different types of impurities. Figs. 19, 20 and 21 show the values for the heat of formation, lattice parameter and bulk modulus, respectively, for all 200 configurations. While there seems to be no particular ordering in the values of the heat of formation, a clear distinction between the different alloys becomes apparent when examining Figs. 20 and 21: different regions can be determined in these plots containing alloys belonging to the four groups studied: Al-Ni-Cu alloys have, for all compositions, the lowest values of the lattice

parameter, followed by Al-Ni and Al-Ni-Cu-Au alloys. Al-Ni-Au alloys have consistently, and not surprisingly, the largest values of the lattice parameter. The same distinction can be made for the bulk modulus, with the exception that now all four groups are more clearly contained in different regions of the diagram, with the Al-Ni alloys having the lowest values of B. As mentioned above, no clear pattern seems to emerge form the heat of formation plot (Fig. 19), however, there is a dominant presence of Al-Ni-Au alloys in the lower region of the diagram, indicating the features described in the previous section with respect to the existence of stable quaternary mixes.

IV. CONCLUDING REMARKS

The results presented in this work can be best summarized by showing the complete set of configurations in one single figure for each bulk property, therefore allowing for comparison of the trends for different types of impurities. Figs. 19, 20 and 21 show the values for the heat of formation, lattice parameter and bulk modulus, respectively, for all 200 configurations. While there seems to be no particular ordering in the values of the heat of formation, a clear distinction between the different alloys becomes apparent when examining Figs. 20 and 21: different regions can be determined in these plots containing alloys belonging to the four groups studied: Al-Ni-Cu alloys have, for all compositions, the lowest values of the lattice parameter, followed by Al-Ni and Al-Ni-Cu-Au alloys. Al-Ni-Au alloys have consistently, and not surprisingly, the largest values of the lattice parameter. The same distinction can be made for the bulk modulus, with the exception that now all four groups are more clearly contained in different regions of the diagram, with the Al-Ni alloys having the lowest values of B. As mentioned above, no clear pattern seems to emerge form the heat of formation plot (Fig. 19), however, there is a dominant presence of Al-Ni-Au alloys in the lower region of the diagram, indicating the features described in the previous section with respect to the existence of stable quaternary mixes.

Although for this initial study the additive elements considered (Cu and Au) to vary the properties of the engineering material (Ni_3Al) might not be optimum, it shows that efficient theoretical methods can go a long way in aiding experimentalists in narrowing the field of viable materials for a particular application. This study focused on three properties, i) stability as exhibited in the heat of formation, ii) strength, as indicated by the bulk modulus and iii) density, as indicated by the change in lattice parameter.

The study demonstrates the effects of concentration and site preference on the above properties of a large number of binary, ternary and quaternary alloys can be studied. Therefore, a prodigious and expensive number of experiments can be narrowed to a much smaller number of promising choices. We find that the following criteria influence the optimum sta-

bility and strength for the alloys examined. In examining off-stoichiometric and non-ordered properties of Ni_3Al, randomizing decreases stability and bulk modulus. Ni- or Al-rich alloys decrease the stability. Ni-rich alloys increase or have a small negative effect on the bulk modulus. Al-rich alloys decrease the bulk modulus. The general effects are a result of the competition between the BFS strain and chemical energy contributions which, due to the numerical simplicity associated with its computation, allows for a speedy and comprehensive study of large number of situations.

Cu additions are characterized by Ni sites substitutions as well as a particular stacking sequence where 1:1 Ni:Al planes alternate with planes containing different numbers of Cu and Ni atoms so as to minimize the number of Cu-Ni bonds. Au additions are also characterized by a Ni site preference but with a different stacking sequence as that found for Al-Ni-Cu alloys. A main feature of the four-component alloys is given by the favorable large contribution to the energy from Cu-Au bonds. Two interesting trends develop: a family of alloys with noticeably low values of ΔH and another with high values of B. Further, there is some evidence for the formation of other ternary phases (Cu-Au-Ni) not included in the current survey.

While most of the predictions and results presented in this work remain to be proven with experimental evidence -keeping in mind that certain restrictions imposed in this calculation would have to be lifted in order to allow for direct comparison with experiment- it is clear that semiempirical methods have achieved the level of development and reliability to warrant examining this new approach to the problem of alloy design. The present work was meant to demonstrate, perhaps in a rather simple way, this power. If not for other advantages, this type of applications of atomistic simulation methods can narrow the gap and improve the feedback between theoretical predictions and laboratory experimentation.

ACKNOWLEDGMENTS

We thank Dr. R. Noebe for many useful discussions and guidance during the development of this project. Fruitful discussions with Dr. N. Bozzolo are gratefully acknowledged. This work was partially supported by the Engineering Directorate, NASA Lewis Research Center.

REFERENCES

[1] Ross, E. W. and Sims, C. S., Superalloys II, Wiley, New York, NY, 1987.

[2] Bozzolo, G., Ferrante J. and Smith, J.R., Phys. Rev. B 45 (1992) 493.

[3] Bozzolo, G. and Ferrante, J., Phys. Rev. B 45 (1992) 12191 .

[4] Bozzolo, G. and Ferrante, J., Scripta Metall. Mater. 26 (1992) 1275.

[5] a. Good, B., Bozzolo, G. and Ferrante, J., Phys. Rev. B 48 (1993) 18284 ; b. Bozzolo, G., Good, B. and Ferrante, J., Surf. Sci. 289 (1993) 169.

[6] Bozzolo, G. and Ferrante, J., Ultramicroscopy 42/44 (1992) 55.

[7] Kobistek, R., Bozzolo, G., Ferrante, J. and Schlosser, H., Surf. Sci. 307/309 (1994) 390.

[8] Bozzolo, G. and Ferrante, J., Phys. Rev. B 46 (1992) 8600.

[9] Bozzolo, G. and Ferrante, J., Phys. Rev. B 50 (1994) 5971.

[10] Bozzolo, G., Ibañez-Meier, R. and Ferrante, J., Phys. Rev. B 51 (1995) 7207.

[11] Bozzolo, G., Ferrante, J. and Kobistek, R., J. Computer-Aided Mater. Des. 1 (1993) 305.

[12] Bozzolo, G. and Ferrante, J., Mater. Res. Soc. Symp. Proc., 291 (1993) 389.

[13] Pearson, W. B., Handbook of Lattice Spacings and Structures of Metals and Alloys, Pergamon Press, Oxford, 1967.

[14] a. Rose, J. H., Smith, J. R. and Ferrante, J., Phys. Rev. B 28 (1983) 1835 ; b. Rose, J. H., Smith, J. R., Guinea, F. and Ferrante, J., Phys. Rev. B 29 (1984) 2963.

[15] Smith, J. R., Perry, T., Banerjea, A., Ferrante, J. and Bozzolo, G., Phys. Rev. B 44 (1991) 6444.

[16] Bozzolo, G., Ferrante, J. and Rodríguez, A. M., J. Computer-Aided Mater. Des. 1 (1993) 285.

[17] Hultgren, R., Orr, R. L., Anderson, P. D. and Kelley, K. K., Selected Values of the Thermodynamic Properties of Binary Alloys, Wiley, New York, 1963.

[18] Carlsson, A. E. and Sanchez, J. M., Solid State Commun. 65 (1988). 527.

APPENDIX

SUBSTITUTIONS AND EXCHANGES ON Ni_3Al

Using the notation introduced in this work, the following list indicates the substitutions ($X \rightarrow Y$) and exchanges ($X \leftrightarrow Y$) on the base alloy Ni_3Al necessary to obtain the alloys studied in this work. The atoms are labeled according to Fig. 1.

1. Ni_3Al
2. $Ni_{B5} \leftrightarrow Al_{A5}$
3. $Ni_{144} \leftrightarrow Al_{A9}$
4. $Ni_{B5} \leftrightarrow Al_{A9}$
5. $(Ni_{B5} \leftrightarrow Al_{A5}) + (Ni_{B9} \leftrightarrow Al_{A9})$
6. $(Ni_{B1} \leftrightarrow Al_{A1}) + (Ni_{B9} \leftrightarrow Al_{A9})$
7. $(Ni_{B4} \leftrightarrow Al_{A5}) + (Ni_{B8} \leftrightarrow Al_{A9})$
8. $Ni_{B3,B4,B7,B8,B11,B12} \leftrightarrow Al_{A1,A2,A5,A6,A9,A10}$
9. $Al_{A5} \rightarrow Ni$
10. $Ni_{B5} \rightarrow Al$
11. $(Ni_{B5} \rightarrow Al) + (Ni_{B8} \leftrightarrow Al_{A6})$
12. $(Ni_{B5} \rightarrow Al) + (Ni_{B3} \leftrightarrow Al_{A2}) + (Ni_{B8} \leftrightarrow Al_{A6})$
13. $(Ni_{B5} \leftrightarrow Al_{C5}) + (Al_{A5} \rightarrow Ni)$
14. $(Al_{A5} \rightarrow Ni) + (Ni_{B5,A7,C7} \leftrightarrow Al_{C5,A6,C6})$
15. $(Ni_{B5} \rightarrow Al) + (Ni_{A3,C3,A7,C7} \leftrightarrow Al_{A5,C5,A6,C6})$
16. $Ni_{B5,D5} \rightarrow Al$
17. $Ni_{B5,B9} \rightarrow Al$
18. $Ni_{B5,B7} \rightarrow Al$
19. $Ni_{B3,B8} \rightarrow Al$
20. $Al_{A5,A9} \rightarrow Ni$
21. $Al_{A5,C5} \rightarrow Ni$

22. $Al_{A1,A6} \rightarrow Ni$

23. $Ni_{B1,B5,B9} \rightarrow Al$

24. $Ni_{B3,B5,B8} \rightarrow Al$

25. $Ni_{B3,B5,B7} \rightarrow Al$

26. $(Ni_{B4,B5,B7} \rightarrow Al)+(Ni_{B3} \leftrightarrow Al_{A5}) + (Ni_{B8} \leftrightarrow Al_{C6})$

27. $(Ni_{B1,B5,B9} \rightarrow Al) + (Ni_{B7} \leftrightarrow Al_{A5}) + (Ni_{B3} \leftrightarrow Al_{C6}) + (Ni_{B8} \leftrightarrow Al_{C5})$

28. $(Ni_{B1,B5,B9} \rightarrow Al) + (Ni_{B3,B7,B8,B11,B12} \leftrightarrow Al_{C6,A5,C5,C10,A9})$

29. $Ni_{C3,C7,C11} \rightarrow Al$

30. $Al_{A1,A5,A9} \rightarrow Ni$

31. $Al_{A5,A6,A9} \rightarrow Ni$

32. $Al_{A1,A6,A9} \rightarrow Ni$

33. $Al_{C5,A6,A9} \rightarrow Ni$

34. $(Al_{A1,A6,A9} \rightarrow Ni + (Ni_{B1} \leftrightarrow Al_{C5})$

35. $(Al_{A5,A6,C6} \rightarrow Ni) + (Al_{C5} \leftrightarrow Ni_{D9}) + (Al_{A9} \leftrightarrow Ni_{B9})$

36. $Ni_{A3,A7,C7} \rightarrow Al$

37. $Ni_{B5,B7,B8,B9} \rightarrow Al$

38. $Ni_{B7,B8,B11,B12} \rightarrow Al$

39. $Ni_{A7,C7,B9,D9} \rightarrow Al$

40. $Ni_{A3,C3,B9,D9} \rightarrow Al$

41. $Al_{A5,C5,A6,C6} \rightarrow Ni$

42. $Al_{A1,A2,C9,C10} \rightarrow Ni$

43. $Al_{A1,C2,C5,A6} \rightarrow Ni$

44. $Al_{A1,C2,A5,C5} \rightarrow Ni$

45. $Ni_{B5} \rightarrow Cu$

46. $(Ni_{B5} \rightarrow Cu) + (Al_{A5,A6} \rightarrow Ni) + (Ni_{B7,B8} \rightarrow Al)$

47. $(Al_{A9,A10} \rightarrow Ni) + (Ni_{B7,B8} \rightarrow Al) + (Ni_{B5} \rightarrow Cu)$

48. $(Ni_{B5} \rightarrow Cu) + (Al_{A5,C5,A6,C6} \rightarrow Ni) + (Ni_{B3,B4,B7,B8} \rightarrow Al)$

49. $(Ni_{B5} \rightarrow Cu) + (Al_{A1,A2,A9,A10} \rightarrow Ni) + (Ni_{B3,B4,B7,B8} \rightarrow Al)$

50. $Al_{A5} \rightarrow Cu$

51. $(Ni_{B5} \leftrightarrow Al_{A5}) + (Al_{A6} \rightarrow Cu)$

52. $(Al_{A9} \rightarrow Cu) + (Al_{A6,A10} \leftrightarrow Ni_{B5,B9})$

53. $(Al_{A6} \rightarrow Cu) + (Al_{C2,C5,C10} \leftrightarrow Ni_{B4,B5,B8})$

54. $(Al_{A6} \rightarrow Cu) + (Al_{C2,C5,C6,C10} \leftrightarrow Ni_{B4,B5,B6,B8})$

55. $(Al_{A6} \rightarrow Cu) + (Al_{A2,A5,C5,C6} \leftrightarrow Ni_{B5,D5,B6,D6})$

56. $(Al_{A5} \rightarrow Cu) + (Ni_{B5} \rightarrow Cu)$

57. $(Al_{C5} \rightarrow Cu) + (Ni_{A7} \rightarrow Cu)$

58. $Ni_{B5,B7} \rightarrow 2Cu$

59. $Ni_{A7,C7} \rightarrow 2Cu$

60. $Ni_{B5,B9} \rightarrow 2Cu$

61. $Al_{A5,A9} \rightarrow Cu$

62. $Al_{A9,C9} \rightarrow 2Cu$

63. $(Al_{A9,C9} \rightarrow 2Cu) + (Al_{C10,A10} \leftrightarrow Ni_{D9,B9})$

64. $(Al_{A9,C9} \rightarrow 2Cu) + (Al_{A5,C5,A10,C10} \leftrightarrow Ni_{B7,D7,B9,D9})$

65. $Ni_{B1,B5,B9} \rightarrow Cu$

66. $Ni_{B1,B5,B7} \rightarrow Cu$

67. $Ni_{B5,B7,B8} \rightarrow Cu$

68. $Ni_{B5,B7,A7} \rightarrow Cu$

69. $(Al_{A5} \rightarrow Cu) + (Ni_{B5,B7} \rightarrow Cu)$

70. $(Al_{A5,A6} \rightarrow Cu) + (Ni_{B5} \rightarrow Cu) + (Ni_{A3,A7} \rightarrow Al)$

71. $(Al_{A5,A6} \rightarrow Cu) + (Ni_{B5} \rightarrow Cu)$

72. $(Al_{A5} \rightarrow Cu) + (Ni_{B5,B7} \rightarrow Cu)$

73. $(Al_{A5,A6} \rightarrow Cu) + (Ni_{B7} \rightarrow Cu)$

74. $Al_{A5,A6,A9} \rightarrow Cu$

75. $Al_{A1,A5,A9} \rightarrow Cu$

76. $(Al_{C1,C5,C9} \leftrightarrow Ni_{B3,B7,B11}) + (Al_{A1,A5,A9} \rightarrow Cu)$

77. $(Ni_{C3,C7,C11} \leftrightarrow Al_{C1,C5,C9}) + (Ni_{B3,B7,B11} \rightarrow Cu)$

78. $(Ni_{B1,B5,B9} \leftrightarrow Al_{C1,C5,C9}) + (Ni_{B3,B7,B11} \rightarrow Cu)$

79. $Ni_{B3,B4,B7,B8} \rightarrow Cu$

80. $Al_{A5,C5,A6,C6} \rightarrow Cu$

81. $Al_{C5,C6,C9,C10} \rightarrow Cu$

82. $Ni_{B5,B7,B8,B9} \rightarrow Cu$

83. $(Ni_{B5,D5} \rightarrow Cu) + (Al_{C5,C6} \rightarrow Cu)$

84. $(Al_{C5,C6} \rightarrow Cu) + (Ni_{C3,C7} \rightarrow Cu)$

85. $(Al_{A5} \rightarrow Cu) + (Ni_{B5,B7,A7} \rightarrow Cu)$

86. $Al_{A5,C5,A6,C6,A9} \rightarrow Cu$

87. $(Al_{A3,C3,A7,C7} \rightarrow Cu) + (Ni_{B5} \rightarrow Cu)$

88. $Al_{A1,C1,A5,C5,A9,C9} \rightarrow Cu$

89. $Al_{A1,C2,A5,C6,A9,C10} \rightarrow Cu$

90. $Ni_{A3,C3,A7,C7,A11,C11} \rightarrow Cu$

91. $Ni_{B1,B3,B5,B7,B9,B11} \rightarrow Cu$

92. $Ni_{A3,C3,B5,D5,A7,C7} \rightarrow Cu$

93. $Ni_{B1,D1,B5,D5,B9,D9} \rightarrow Cu$

94. $Ni_{B3,B4,B7,B8,B11,B12} \rightarrow Cu$

95. $(Al_{A5,A6} \rightarrow Cu) + (Ni_{A3,C3,A7,C7} \rightarrow Cu)$

96. $(Al_{A5,C5,A6,C6} \rightarrow Cu) + (Ni_{B5,D5} \rightarrow Cu)$

97. $(Al_{A5,C5,A6,C6} \rightarrow Cu) + (Ni_{B1,B9} \rightarrow Cu)$

98. $(Al_{C1,A2,C9,A10} \rightarrow Cu) + (Ni_{B3,B8} \rightarrow Cu)$

99. $Ni_{B1,B3,B4,B5,B7,B8,B9,B11,B12} \rightarrow Cu$

100. $Al_{A1,C2,A5,C5,A6,C6,C9,A10} \rightarrow Cu$

101. $Ni_{B5} \rightarrow Au$

102. $(Ni_{B5} \rightarrow Au) + (Al_{A5,A6} \rightarrow Ni) + (Ni_{B7,B8} \rightarrow Al)$

103. $(Al_{A9,A10} \rightarrow Ni) + (Ni_{B7,B8} \rightarrow Al) + (Ni_{B5} \rightarrow Au)$

104. $(Ni_{B5} \rightarrow Au) + (Al_{A5,C5,A6,C6} \rightarrow Ni) + (Ni_{B3,B4,B7,B8} \rightarrow Al)$

105. $(Ni_{B5} \rightarrow Au) + (Al_{A1,A2,A9,A10} \rightarrow Ni) + (Ni_{B3,B4,B7,B8} \rightarrow Al)$

106. $Al_{A5} \rightarrow Au$

107. $(Ni_{B5} \leftrightarrow Al_{A5}) + (Al_{A6} \rightarrow Au)$

108. $(Al_{A9} \rightarrow Au) + (Al_{A6,A10} \leftrightarrow Ni_{B5,B9})$

109. $(Al_{A6} \rightarrow Au) + (Al_{C2,C5,C10} \leftrightarrow Ni_{B4,B5,B8})$

110. $(Al_{A6} \rightarrow Au) + (Al_{C2,C5,C6,C10} \leftrightarrow Ni_{B4,B5,B6,B8})$

111. $(Al_{A6} \rightarrow Au) + (Al_{A2,A5,C5,C6} \leftrightarrow Ni_{B5,D5,B6,D6})$

112. $(Al_{A5} \rightarrow Au) + (Ni_{B5} \rightarrow Au)$

113. $(Al_{C5} \rightarrow Au) + (Ni_{A7} \rightarrow Au)$

114. $Ni_{B5,B7} \rightarrow 2Au$

115. $Ni_{A7,C7} \rightarrow 2Au$

116. $Ni_{B5,B9} \rightarrow 2Au$

117. $Al_{A5,A9} \rightarrow Au$

118. $Al_{A9,C9} \rightarrow 2Au$

119. $(Al_{A9,C9} \rightarrow 2Au) + (Al_{C10,A10} \leftrightarrow Ni_{D9,B9})$

120. $(Al_{A9,C9} \rightarrow 2Au) + (Al_{A5,C5,A10,C10} \leftrightarrow Ni_{B7,D7,B9,D9})$

121. $Ni_{B1,B5,B9} \rightarrow Au$

122. $Ni_{B1,B5,B7} \rightarrow Au$

123. $Ni_{B5,B7,B8} \rightarrow Au$

124. $Ni_{B5,B7,A7} \rightarrow Au$

125. $(Al_{A5} \rightarrow Au) + (Ni_{B5,B7} \rightarrow Au)$

126. $(Al_{A5,A6} \rightarrow Au) + (Ni_{B5} \rightarrow Au) + (Ni_{A3,A7} \rightarrow Al)$

127. $(Al_{A5,A6} \rightarrow Au) + (Ni_{B5} \rightarrow Au)$

128. $(Al_{A5} \rightarrow Au) + (Ni_{B5,B7} \rightarrow Au)$

129. $(Al_{A5,A6} \rightarrow Au) + (Ni_{B7} \rightarrow Au)$

130. $Al_{A5,A6,A9} \rightarrow Au$

131. $Al_{A1,A5,A9} \rightarrow Au$

132. $(Al_{C1,C5,C9} \leftrightarrow Ni_{B3,B7,B11}) + (Al_{A1,A5,A9} \rightarrow Au)$

133. $(Ni_{C3,C7,C11} \leftrightarrow Al_{C1,C5,C9}) + (Ni_{B3,B7,B11} \rightarrow Au)$

134. $(Ni_{B1,B5,B9} \leftrightarrow Al_{C1,C5,C9}) + (Ni_{B3,B7,B11} \rightarrow Au)$

135. $Ni_{B3,B4,B7,B8} \rightarrow Au$

136. $Al_{A5,C5,A6,C6} \rightarrow Au$

137. $Al_{C5,C6,C9,C10} \rightarrow Au$

138. $Ni_{B5,B7,B8,B9} \rightarrow Au$

139. $(Ni_{B5,D5} \rightarrow Au) + (Al_{C5,C6} \rightarrow Au)$

140. $(Al_{C5,C6} \rightarrow Au) + (Ni_{C3,C7} \rightarrow Au)$

141. $(Al_{A5} \rightarrow Au) + (Ni_{B5,B7,A7} \rightarrow Au)$

142. $Al_{A5,C5,A6,C6,A9} \rightarrow Au$

143. $(Al_{A3,C3,A7,C7} \rightarrow Au) + (Ni_{B5} \rightarrow Au)$

144. $Al_{A1,C1,A5,C5,A9,C9} \rightarrow Au$

145. $Al_{A1,C2,A5,C6,A9,C10} \rightarrow Au$

146. $Ni_{A3,C3,A7,C7,A11,C11} \rightarrow Au$

147. $Ni_{B1,B3,B5,B7,B9,B11} \rightarrow Au$

148. $Ni_{A3,C3,B5,D5,A7,C7} \rightarrow Au$

149. $Ni_{B1,D1,B5,D5,B9,D9} \rightarrow Au$

150. $Ni_{B3,B4,B7,B8,B11,B12} \rightarrow Au$

151. $(Al_{A5,A6} \rightarrow Au) + (Ni_{A3,C3,A7,C7} \rightarrow Au)$

152. $(Al_{A5,C5,A6,C6} \rightarrow Au) + (Ni_{B5,D5} \rightarrow Au)$

153. $(Al_{A5,C5,A6,C6} \rightarrow Au) + (Ni_{B1,B9} \rightarrow Au)$

154. $(Al_{C1,A2,C9,A10} \rightarrow Au) + (Ni_{B3,B8} \rightarrow Au)$

155. $Ni_{B1,B3,B4,B5,B7,B8,B9,B11,B12} \rightarrow Au$

156. $Al_{A1,C2,A5,C5,A6,C6,C9,A10} \rightarrow Au$

157. $(Ni_{B5} \rightarrow Cu) + (Ni_{B7} \rightarrow Au)$

158. $(Ni_{B5} \rightarrow Cu) + (Ni_{B9} \rightarrow Au)$

159. $(Al_{A5} \rightarrow Cu) + (Al_{A9} \rightarrow Au)$

160. $(Al_{A1} \rightarrow Cu) + (Ni_{B9} \rightarrow Au)$

161. $(Al_{A5} \rightarrow Au) + (Ni_{B5} \rightarrow Cu)$

162. $(Ni_{A7} \rightarrow Cu) + (Ni_{C7} \rightarrow Au)$

163. $(Al_{A5} \rightarrow Cu) + (Al_{C5} \rightarrow Au)$

164. $(Al_{C5,A6} \rightarrow Cu) + (Al_{A5,C6} \rightarrow Au)$

165. $(Ni_{A7,C3} \rightarrow Cu) + (Ni_{A3,C7} \rightarrow Au)$

166. $(Ni_{A3,C7,A11} \rightarrow Cu) + (Ni_{C3,A7,C11} \rightarrow Au)$

167. $(Al_{A1,C5,A9} \rightarrow Cu) + (Al_{C1,A5,C9} \rightarrow Au)$

168. $(Ni_{B3,B4,B7,B8,B11,B12} \rightarrow Au) + (Ni_{B1,B5,B9} \rightarrow Cu)$

169. $(Ni_{B1,D1,B5,D5,B9,D9} \rightarrow Cu) + (Ni_{B3,D3,B4,D4,B7,D7,B8,D8,B11,D11,B12,D12} \rightarrow Au)$

170. $(Ni_{D1,D2,D5,D6,D9,D10} \rightarrow Cu) + (Ni_{D3,D4,D7,D8,D11,D12} \rightarrow Au)$

171. $(Ni_{B1,D2,B5,D6,B9,D10} \rightarrow Cu) + (Ni_{B3,D3,B4,D4,B7,D7,B8,D8,B11,D11,B12,D12} \rightarrow Au)$

172. $(Ni_{B1,D1,B2,D2,B5,D5,B6,D6,B9,D9,B10,D10} \rightarrow Cu) +$
$(Ni_{B3,D3,B4,D4,B7,D7,B8,D8,B11,D11,B12,D12} \rightarrow Au)$

173. $(Ni_{B1,B5,B7,C3,C4,C7,C8,C11,C12} \rightarrow Au) + (Al_{A1,A5,A7,C2,C4,C6} \rightarrow Cu) +$
$(Al_{A2,A6,A10} \rightarrow Au)$

174. $(Al_{A1,A5,A9,C2,C6,C10} \rightarrow Cu) + (Al_{A2,A10,C5} \rightarrow Au) +$
$(Ni_{A3,A7,A11,C3,C7,C11,D1,D5,D9} \rightarrow Au)$

175. $(Al_{A2,A5,A10} \rightarrow Ni) + (Al_{A1,A6,A9,C2,C5,C10} \rightarrow Cu) +$
$(Ni_{B3,B4,B7,B8,B11,B12,D1,D2,D5,D6,D9,D10} \rightarrow Au)$

176. $(Al_{A,C} \rightarrow Au) + (Ni_{A3,A7,A11,D1,D5,D9} \rightarrow Cu) + (Ni_{B1,B5,B9} \rightarrow Al)$

177. $(Al_{A1,A2,A5,A6,A9,A10,C2,C6,C10} \rightarrow Ni) + (Ni_{B3,B4,B7,B8,B11,B12} \rightarrow Cu) +$
$(Ni_{B1,B2,B5,B6,B9,B10,C3,C4,C7,C8,C11,C12} \rightarrow Au)$

178. $(Al_{C1,C2,C5,C6,C9,C10} \rightarrow Cu) + (Ni_B \rightarrow Au)$

179. $(Al \rightarrow Cu) + (Ni_{A3,A7,B3,B4,B7,B8,C3,C7,D3,D4,D7,D8} \rightarrow Au)$

180. $(Al_C \rightarrow Au) + (Ni_{B1,B5,B9,D2,D6,D10} \rightarrow Cu) + (Ni_{B2,B6,B10,D1,D5,D9} \rightarrow Au)$

181. $(Al_C \rightarrow Ni) + (Ni_A \rightarrow Cu) + (Ni_{B3,B4,B7,B8,B11,B12,D3,D4,D7,D8,D11,D12} \rightarrow Au)$

182. $(Ni_{A,C} \rightarrow Au) + (Al_C \rightarrow Ni) + (Ni_{B1,B5,B9,D2,D6,D10} \rightarrow Cu)$

183. $(Al_{A1,A5,A9,C2,C6,C10} \rightarrow Cu) + (Ni_{A,C} \rightarrow Au)$

184. $(Al_{A5,A6,C1,C2,C9,C10} \rightarrow Cu) + (Ni_{A,C} \rightarrow Au)$

185. $(Al_{A2,A5,A10,C1,C6,C9} \rightarrow Cu)+(Ni_{A,C} \rightarrow Au)$

186. $(Al_{A2,A5,A10,C1,C6,C9} \rightarrow Cu)+(Ni_{B1,B2,B5,B6,B9,B10,D3,D4,D7,D8,D11,D12} \rightarrow Au)$

187. $(Al_{C} \rightarrow Cu)+(Ni_{A,C} \rightarrow Au)$

188. $(Al_{A5,A6,C1,C2,C9,C10} \rightarrow Cu)+(Ni_{B3,B4,B7,B8,B11,B12,C3,C4,C7,C8,C11,C12} \rightarrow Au)$

189. $(Al_{C} \rightarrow Cu)+(Ni_{B1,B2,B5,B6,B9,B10,D1,D2,D5,D6,D9,D10} \rightarrow Au)$

190. $(Al_{C} \rightarrow Ni)+(Ni_{B1,B5,B9,D1,D5,D9} \rightarrow Cu) + (Ni_{B2,B6,B10,D2,D6,D10} \rightarrow Al) +$
$(Ni_{B3,B4,B7,B8,B11,B12,D3,D4,D7,D8,D11,D12} \rightarrow Au)$

191. $(Al_{A} \rightarrow Ni)+(Ni_{A3,A7,A11,C4,C8,C12} \rightarrow Cu) + (Ni_{C3,C7,C11} \rightarrow Al)+$
$(Ni_{B3,B4,B7,B8,B11,B12,D3,D4,D7,D8,D11,D12} \rightarrow Au)$

192. $(Al_{A2,A5,A10,C1,C6,C9} \rightarrow Ni)+(Ni_{A3,A7,A11,C3,C7,C11} \rightarrow Cu)+$
$(Ni_{D2,D6,D10} \rightarrow Al) +(Ni_{B1,B2,B5,B6,B9,B10,C4,C8,C12,D1,D5,D9} \rightarrow Au)$

193. $(Al_{C} \rightarrow Ni)+(Ni_{A} \rightarrow Au)+(Ni_{B1,B5,B9,C3,C7,C11} \rightarrow Cu) +$
$(Ni_{D3,D4,D7,D8,D11,D12} \rightarrow Au)$

194. $(Al_{A} \rightarrow Cu)+(Al_{C} \rightarrow Ni)+(Ni_{B4,B8,B12,C3,C7,C11} \rightarrow Al)+$
$(Ni_{B1,B2,B5,B6,B9,B10,D1,D2,D5,D6,D9,D10} \rightarrow Au)$

195. $(Al_{A} \rightarrow Cu)+(Ni_{A3,A7,A11} \rightarrow Al)+$
$(Ni_{B3,B4,B7,B8,B11,B12,D1,D2,D5,D6,D9,D10} \rightarrow Au)$

196. $(Al_{C} \rightarrow Cu)+(Ni_{C3,C7,C11} \rightarrow Al)+$
$(Ni_{B3,B4,B7,B8,B11,B12,D3,D4,D7,D8,D11,D12} \rightarrow Au)$

197. $(Ni_{A4,A8,A12,B1,B5,B9,C3,C7,C11,D1,D5,D9} \rightarrow Au)+(Ni_{A3,A7,A11,C4,C8,C12} \rightarrow Cu)$

198. $(Ni_{A} \rightarrow Cu)+(Ni_{B3,B4,B7,B8,B11,B12,D1,D2,D5,D6,D9,D10} \rightarrow Au)$

199. $(Ni_{A3,A7,A11,C3,C7,C11} \rightarrow Cu)+ (Ni_{B3,B4,B7,B8,B11,B12,D3,D4,D7,D8,D11,D12} \rightarrow Au)$

200. $(Ni_{B1,B2,B5,B6,B9,B10} \rightarrow Cu)+ (Ni_{B3,B4,B7,B8,B11,B12,D3,D4,D7,D8,D11,D12} \rightarrow Au)$

Table 1: Experimental input: cohesive energy (in eV) and lattice parameter (in Å). ECT parameters: p, l (in Å), α (in Å^{-1}) and λ (in Å) for the elements considered in this work.

ECT PARAMETERS AND EXPERIMENTAL INPUT						
Element	Cohesive Energy	Lattice Constant	p	l	α	λ
Al	3.34	4.05	4	0.336	2.105	0.944
Cu	3.50	3.615	6	0.272	2.935	0.765
Au	3.78	4.078	10	0.236	4.339	0.663
Ni	4.435	3.524	6	0.270	3.015	0.759

Table 2: BFS parameters Δ_{AB} and Δ_{BA} (in Å^{-1}) and heats of solution in the dilute limit E^{sol}_{AB} and E^{sol}_{BA} (in eV/atom) for all the possible combinations of Ni, Al, Cu and Au. The values for Al-Ni were obtained from [1] a theoretical calculation by Sanchez and Carlsson [18] and by [2] fitting to the experimental values of the heat of formation and lattice parameter of the ordered Ni_3Al $L1_2$ structure.

BFS PARAMETERS Δ_{AB} AND Δ_{BA} (IN Å^{-1})				
A-B	Δ_{AB}	Δ_{BA}	E^{sol}_{AB}	E^{sol}_{BA}
Al-Au	-0.0501	-0.0853	-1.26	-0.80
Al-Cu	-0.0526	-0.0626	-0.35	-0.20
Al-Ni[1]	-0.0657	-0.0861	-1.715	-0.494
Al-Ni[2]	-0.06564	-0.08613		
Au-Cu	-0.0513	-0.0604	-0.191	-0.126
Au-Ni	-0.0506	-0.0622	0.280	0.218
Cu-Ni	-0.0163	0.0309	0.100	0.032

Table 3: Bulk parameters of Al-Ni alloys. The first columns indicates the configuration number (see a graphical description of these configurations in Figs. 1, 2 and 8 and in Appendix 1). The next column indicates the heat of formation (in eV/atom) of the rigid structure, i.e., when the lattice parameter is that of the ground state Ni_3Al alloy. The third column indicate the relaxed heat of formation (in eV/atom) (relative to the rigid Ni_3Al $L1_2$ structure). The next three columns list the cohesive energy (in eV) per particle, the lattice parameter (in Å) and the universal binding energy curve parameter l, from which the bulk modulus (B) can be extracted, as listed in the last column.

BULK PROPERTIES OF Al-Ni ALLOYS						
Conf.	ΔH_{rigid}	$\Delta H_{relaxed}$	E_c	a	l	B
(-4, 4, 0, 0)						
37	-0.26721	-0.27705	4.3470	3.6123	0.292	153.13
39	-0.27123	-0.28085	4.3508	3.6118	0.292	153.29
40	-0.29967	-0.30728	4.3777	3.6075	0.292	154.49
36	-0.30802	-0.31523	4.3855	3.6060	0.292	154.84
38	-0.30802	-0.31523	4.3855	3.6060	0.292	154.84
(-3, 3, 0, 0)						
28	-0.08161	-0.10021	4.1930	3.6311	0.291	148.33
27	-0.14982	-0.16350	4.2563	3.6212	0.291	150.99
26	-0.23455	-0.24315	4.3359	3.6090	0.291	154.38
24	-0.29999	-0.30546	4.3983	3.5997	0.291	157.05
25	-0.30240	-0.30778	4.4006	3.5993	0.291	157.14
23	-0.31992	-0.32452	4.4173	3.5966	0.291	157.86
29	-0.32522	-0.32965	4.4225	3.5959	0.291	158.07

Table 3 (continued):

BULK PROPERTIES OF Al-Ni ALLOYS						
Conf.	ΔH_{rigid}	$\Delta H_{relaxed}$	E_c	a	l	B
(-2, 2, 0, 0)						
18	-0.33197	-0.33437	4.4500	3.5871	0.289	161.01
19	-0.34041	-0.34256	4.4582	3.5859	0.289	161.37
17	-0.34150	-0.34362	4.4592	3.5857	0.289	161.43
16	-0.34728	-0.34925	4.4649	3.5849	0.289	161.63
(-1, 1, 0, 0)						
15	-0.23455	-0.23822	4.3766	3.5929	0.288	159.63
12	-0.26816	-0.27081	4.4092	3.5884	0.288	161.01
11	-0.31744	-0.31882	4.4572	3.5813	0.288	163.10
10	-0.36533	-0.36588	4.5043	3.5745	0.288	165.19
(0, 0, 0, 0)						
8	-0.20002	-0.20290	4.3641	3.5894	0.286	160.91
7	-0.26151	-0.26288	4.4241	3.5812	0.286	163.50
5	-0.28991	-0.29074	4.4520	3.5772	0.286	164.69
6	-0.28991	-0.29074	4.4520	3.5772	0.286	164.69
4	-0.32567	-0.32602	4.4873	3.5722	0.286	166.25
3	-0.32660	-0.32694	4.4882	3.5721	0.286	166.30
2	-0.33982	-0.34004	4.5013	3.5703	0.286	166.86
1	-0.39142	-0.39142	4.5527	3.5631	0.286	169.12

Table 3 (concluded):

BULK PROPERTIES OF Al-Ni ALLOYS						
Conf.	ΔH_{rigid}	$\Delta H_{relaxed}$	E_c	a	l	B
(1,-1, 0, 0)						
14	-0.25469	-0.25521	4.4393	3.5742	0.285	166.00
13	-0.31793	-0.31795	4.5020	3.5655	0.285	168.74
9	-0.35269	-0.35271	4.5368	3.5607	0.285	170.28
(2,-2, 0, 0)						
22	-0.31470	-0.31481	4.5217	3.5581	0.284	171.51
20	-0.31532	-0.31543	4.5223	3.5580	0.284	171.53
21	-0.31667	-0.31679	4.5237	3.5578	0.284	171.57
(3,-3, 0, 0)						
35	-0.18753	-0.18762	4.4173	3.5676	0.282	168.77
34	-0.22701	-0.22702	4.4567	3.5624	0.282	170.49
32	-0.27807	-0.27833	4.5080	3.5554	0.282	172.80
33	-0.27820	-0.27846	4.5081	3.5554	0.282	172.80
30	-0.27930	-0.27956	4.5092	3.5552	0.282	172.85
31	-0.27991	-0.28018	4.5099	3.5551	0.282	172.90
(4,-4, 0, 0)						
43	-0.24341	-0.24390	4.4964	3.5524	0.281	174.21
44	-0.24341	-0.24390	4.4964	3.5524	0.281	174.21
42	-0.24341	-0.24391	4.4964	3.5523	0.281	174.19
41	-0.24931	-0.24991	4.5024	3.5513	0.281	174.48

Table 4: Same as in Table 1 for Al-Ni-Cu alloys.

BULK PROPERTIES OF Al-Ni-Cu ALLOYS						
(-9, 0, 9, 0)						
99	-0.29271	-0.29658	4.2825	3.5939	0.287	156.85
(-6, 0, 6, 0)						
91	-0.32512	-0.32683	4.3712	3.5835	0.287	160.86
92	-0.32522	-0.32694	4.3713	3.5835	0.287	160.86
90	-0.32828	-0.32991	4.3743	3.5829	0.287	161.02
93	-0.32828	-0.32991	4.3743	3.5829	0.287	161.02
94	-0.32828	-0.32991	4.3743	3.5829	0.287	161.02
(-5, 0, 5, 0)						
87	-0.33655	-0.33773	4.4016	3.5800	0.287	162.26
(-4, 0, 4, 0)						
82	-0.34667	-0.34744	4.4308	3.5767	0.287	163.55
79	-0.34852	-0.34926	4.4326	3.5763	0.287	163.65
(-4,-2, 6, 0)						
95	-0.28504	-0.28546	4.3755	3.5731	0.284	164.72
(-3, 0, 3, 0)						
78	-0.21743	-0.22111	4.3239	3.5930	0.287	158.98
77	-0.27124	-0.27329	4.3761	3.5853	0.287	161.27
70	-0.30540	-0.30667	4.4095	3.5806	0.287	162.68
68	-0.35761	-0.35804	4.4608	3.5733	0.287	164.93
69	-0.35761	-0.35804	4.4608	3.5733	0.287	164.93
67	-0.35806	-0.35849	4.4613	3.5732	0.287	164.96
66	-0.35820	-0.35862	4.4614	3.5732	0.287	164.96
65	-0.35864	-0.35906	4.4619	3.5731	0.287	165.01

Table 4 (continued):

BULK PROPERTIES OF Al-Ni-Cu ALLOYS						
Conf.	ΔH_{rigid}	$\Delta H_{relaxed}$	E_c	a	l	B
(-3,-1, 4, 0)						
85	-0.32981	-0.33008	4.4362	3.5711	0.285	165.67
(-2, 0, 2, 0)						
60	-0.36947	-0.36965	4.4919	3.5697	0.287	166.34
58	-0.36954	-0.36972	4.4920	3.5697	0.287	166.36
59	-0.36957	-0.36975	4.4920	3.5697	0.287	166.34
(-2,-1, 3, 0)						
72	-0.33779	-0.33789	4.4635	3.5681	0.285	166.89
(-2,-2, 4, 0)						
84	-0.30754	-0.30758	4.4365	3.5663	0.284	167.52
83	-0.30788	-0.30792	4.4369	3.5662	0.284	167.53
(-2,-4, 6, 0)						
97	-0.22231	-0.22234	4.3580	3.5660	0.281	167.64
98	-0.22546	-0.22549	4.3611	3.5657	0.281	167.84
96	-0.24806	-0.24807	4.3837	3.5623	0.281	168.86
(-1, 0, 1, 0)						
49	-0.18548	-0.18931	4.3311	3.5935	0.287	159.39
48	-0.24487	-0.24692	4.3887	3.5853	0.287	161.90
47	-0.27589	-0.27724	4.4190	3.5810	0.287	163.21
46	-0.28329	-0.28447	4.4262	3.5799	0.287	163.53
45	-0.38039	-0.38044	4.5222	3.5664	0.287	167.73

Table 4 (continued):

BULK PROPERTIES OF Al-Ni-Cu ALLOYS						
(-1,-1, 2, 0)						
57	-0.34161	-0.34164	4.4867	3.5658	0.285	167.98
56	-0.34544	-0.34546	4.4906	3.5652	0.285	168.13
(-1,-2, 3, 0)						
73	-0.30835	-0.30836	4.4568	3.5644	0.284	168.48
71	-0.31182	-0.31182	4.4602	3.5639	0.284	168.64
(0,-1, 1, 0)						
54	-0.21613	-0.21756	4.3821	3.5815	0.285	163.41
53	-0.21777	-0.21918	4.3837	3.5814	0.285	163.49
52	-0.26640	-0.26694	4.4315	3.5744	0.285	165.60
51	-0.31654	-0.31662	4.4812	3.5675	0.285	167.77
55	-0.34221	-0.34221	4.5068	3.5639	0.285	168.91
50	-0.35295	-0.35295	4.5175	3.5624	0.285	169.37
(0,-2, 2, 0)						
64	-0.25784	-0.25802	4.4259	3.5697	0.284	167.15
63	-0.30737	-0.30737	4.4753	3.5626	0.284	169.35
61	-0.31530	-0.31531	4.4832	3.5616	0.284	169.71
62	-0.31612	-0.31613	4.4840	3.5615	0.284	169.71
(0,-3, 3, 0)						
76	-0.26534	-0.26535	4.4366	3.5624	0.282	169.47
75	-0.27847	-0.27849	4.4497	3.5607	0.282	170.06
74	-0.27886	-0.27888	4.4501	3.5607	0.283	170.06

Table 4 (concluded):

BULK PROPERTIES OF Al-Ni-Cu ALLOYS						
(0,-4, 4, 0)						
81	-0.24312	-0.24317	4.4177	3.5595	0.281	170.49
80	-0.24542	-0.24549	4.4201	3.5591	0.281	170.60
(0,-5, 5, 0)						
86	-0.20856	-0.20866	4.3866	3.5582	0.280	170.95
(0,-6, 6, 0)						
89	-0.16826	-0.16837	4.3496	3.5579	0.279	171.15
88	-0.17242	-0.17257	4.3538	3.5572	0.279	171.34
(0,-8, 8, 0)						

Table 5: Same as in Table 1 for Al-Ni-Au alloys.

BULK PROPERTIES OF Al-Ni-Au ALLOYS						
Conf.	ΔH_{rigid}	$\Delta H_{relaxed}$	E_c	a	l	B
(-9, 0, 0, 9)						
155	-0.15633	-0.31998	4.3584	3.7374	0.271	172.71
(-6, 0, 0, 6)						
148	-0.22979	-0.31238	4.3917	3.6914	0.275	170.90
147	-0.25394	-0.33203	4.4114	3.6878	0.275	171.86
146	-0.37184	-0.42981	4.5092	3.6703	0.275	176.65
149	-0.37184	-0.42981	4.5092	3.6703	0.275	176.65
150	-0.37184	-0.42981	4.5092	3.6703	0.275	176.65
(-5, 0, 0, 5)						
143	-0.29930	-0.35235	4.4454	3.6672	0.276	172.22
(-4, 0, 0, 4)						
138	-0.30008	-0.33789	4.4445	3.6522	0.278	170.80
135	-0.37534	-0.40366	4.5103	3.6401	0.278	173.96
(-4,-2, 0, 6)						
151	-0.24295	-0.30498	4.4300	3.6737	0.273	176.32
(-3, 0, 0, 3)						
134	-0.21932	-0.24875	4.3691	3.6432	0.280	166.10
125	-0.27577	-0.30177	4.4221	3.6382	0.280	168.37
126	-0.27704	-0.30232	4.4226	3.6372	0.280	168.45
133	-0.28335	-0.30700	4.4273	3.6348	0.280	168.72
124	-0.31973	-0.34231	4.4626	3.6329	0.280	170.15

Table 5 (continued):

BULK PROPERTIES OF Al-Ni-Au ALLOYS						
Conf.	ΔH_{rigid}	$\Delta H_{relaxed}$	E_c	a	l	B
(-3, 0, 0, 3)						
123	-0.33887	-0.35947	4.4798	3.6298	0.280	170.98
122	-0.35541	-0.37433	4.4946	3.6270	0.280	171.71
121	-0.37709	-0.39394	4.5142	3.6233	0.280	172.62
(-3,-1, 0, 4)						
141	-0.24727	-0.28525	4.4147	3.6523	0.277	171.16
(-2, 0, 0, 2)						
114	-0.36018	-0.36950	4.5034	3.6086	0.282	170.48
116	-0.38064	-0.38831	4.5225	3.6050	0.282	171.45
115	-0.38187	-0.38948	4.5237	3.6048	0.282	171.48
(-2,-1, 0, 3)						
128	-0.29680	-0.31646	4.4596	3.6281	0.279	171.83
(-2,-2, 0, 4)						
140	-0.24960	-0.28065	4.4329	3.6435	0.276	173.82
139	-0.25021	-0.28119	4.4335	3.6434	0.276	173.88
(-2,-4, 0, 6)						
152	-0.12708	-0.19117	4.3618	3.6753	0.270	176.55
154	-0.21251	-0.26287	4.4335	3.6624	0.270	180.16
153	-0.24743	-0.29260	4.4632	3.6571	0.270	181.62

Table 5 (continued):

BULK PROPERTIES OF Al-Ni-Au ALLOYS						
Conf.	ΔH_{rigid}	$\Delta H_{relaxed}$	E_c	a	l	B
(-1, 0, 0, 1)						
105	-0.18109	-0.19171	4.3393	3.6128	0.284	161.60
104	-0.24490	-0.25190	4.3997	3.6039	0.284	164.30
103	-0.27687	-0.28270	4.4303	3.5998	0.284	165.59
102	-0.29049	-0.29566	4.4432	3.5976	0.284	166.16
101	-0.38541	-0.38751	4.5351	3.5850	0.284	170.21
(-1,-1, 0, 2)						
112	-0.33486	-0.34224	4.4992	3.6040	0.281	172.17
113	-0.35213	-0.35855	4.5154	3.6009	0.281	172.94
(-1,-2, 0, 3)						
127	-0.28530	-0.30113	4.4671	3.6213	0.277	174.06
129	-0.30152	-0.31590	4.4818	3.6185	0.277	174.77
(0,-1, 0, 1)						
110	-0.21551	-0.22148	4.3919	3.6003	0.283	165.70
109	-0.21841	-0.22425	4.3947	3.5999	0.283	165.82
108	-0.26972	-0.27350	4.4439	3.5925	0.283	168.02
107	-0.31973	-0.32200	4.4924	3.5859	0.283	170.18
111	-0.34698	-0.34865	4.5191	3.5826	0.283	171.33
106	-0.35849	-0.35983	4.5302	3.5805	0.283	171.87

Table 5 (concluded):

BULK PROPERTIES OF Al-Ni-Au ALLOYS						
Conf.	ΔH_{rigid}	$\Delta H_{relaxed}$	E_c	a	l	B
(0,-2, 0, 2)						
120	-0.26059	-0.26861	4.4485	3.6060	0.279	171.76
119	-0.31391	-0.31963	4.4992	3.5986	0.279	174.01
118	-0.32549	-0.33058	4.5101	3.5966	0.279	174.53
117	-0.32553	-0.33062	4.5102	3.5965	0.279	174.54
(0,-3, 0, 3)						
132	-0.27516	-0.28742	4.4762	3.6142	0.276	176.36
131	-0.29253	-0.30345	4.4922	3.6113	0.276	177.14
130	-0.29258	-0.30349	4.4922	3.6113	0.276	177.13
(0,-4, 0, 4)						
137	-0.25958	-0.27814	4.4760	3.6249	0.273	179.68
136	-0.25960	-0.27815	4.4761	3.6249	0.273	179.70
(0,-5, 0, 5)						
142	-0.22674	-0.25450	4.4616	3.6376	0.270	182.22
(0,-6, 0, 6)						
144	-0.19370	-0.23207	4.4483	3.6494	0.268	184.64
145	-0.19395	-0.23231	4.4485	3.6494	0.268	184.62
(0,-8, 0, 8)						
156	-0.12856	-0.19164	4.4262	3.6707	0.263	189.46

Table 6: Same as in Table 1 for Al-Ni-Cu-Au alloys.

BULK PROPERTIES OF Al-Ni-Cu-Au ALLOYS						
Conf.	ΔH_{rigid}	$\Delta H_{relaxed}$	E_c	a	l	B
(-9, 0, 3, 6)						
168	-0.32369	-0.39321	4.4141	3.6812	0.275	172.17
(-6, 0, 3, 3)						
166	-0.34615	-0.36819	4.4300	3.6324	0.280	168.72
(-4, 0, 2, 2)						
165	-0.35992	-0.37026	4.4653	3.6112	0.282	168.76
(-2, 0, 1, 1)						
157	-0.37300	-0.37581	4.5039	3.5885	0.284	168.78
158	-0.37474	-0.37749	4.5056	3.6882	0.284	168.87
162	-0.37510	-0.37783	4.5059	3.5882	0.284	168.88
(-1, -1, 1, 1)						
160	-0.34641	-0.34841	4.4993	3.5845	0.283	170.43
161	-0.35007	-0.35188	4.5028	3.5834	0.283	170.63
(0, -2, 1, 1)						
159	-0.32022	-0.32146	4.4952	3.5799	0.281	172.12
163	-0.32042	-0.32165	4.4954	3.5798	0.281	172.12
(0, -4, 2, 2)						
164	-0.25111	-0.25574	4.4420	3.5949	0.277	175.08
(0, -6, 3, 3)						
167	-0.18114	-0.19105	4.3898	3.6089	0.273	177.89
(0,-12, 6, 6)						
170	-0.27773	-0.35923	4.3217	3.6920	0.275	167.85

Table 6 (continued):

BULK PROPERTIES OF Al-Ni-Cu-Au ALLOYS						
Conf.	ΔH_{rigid}	$\Delta H_{relaxed}$	E_c	a	l	B
(0,-18, 6,12)						
197	-0.08596	-0.36085	4.2414	3.7837	0.2674	170.20
171	-0.28357	-0.50175	4.3823	3.7588	0.2673	177.24
200	-0.28361	-0.50178	4.3824	3.7588	0.2673	177.26
169,199	-0.28511	-0.50291	4.3835	3.7586	0.267	177.29
198	-0.28736	-0.50474	4.3853	3.7584	0.2673	177.41
(-3,-15,6,12)						
191	-0.01244	-0.25133	4.2004	3.7685	0.2640	173.62
192	-0.00813	-0.25420	4.2032	3.7712	0.2641	173.50
193	-0.00429	-0.26000	4.2090	3.7748	0.2642	173.42
194	-0.11053	-0.32793	4.2770	3.7583	0.2640	177.27
195	-0.22053	-0.41563	4.3647	3.7472	0.2641	181.42
196	-0.22247	-0.41713	4.3661	3.7470	0.2641	181.47
(-6,-12,6,12)						
178	0.22163	-0.05553	4.0730	3.7833	0.2611	171.54
179	0.10826	-0.13590	4.1534	3.7692	0.2610	175.66
180	0.05717	-0.17059	4.1880	3.7620	0.2609	177.54
181	-0.07405	-0.26354	4.2810	3.7442	0.2608	182.51
182	-0.10895	-0.29156	4.3090	3.7406	0.2608	183.87
183	-0.15955	-0.33221	4.3497	3.7354	0.2609	185.85
184	-0.15993	-0.33248	4.3499	3.7353	0.2609	185.84
185	-0.15991	-0.33250	4.3500	3.7353	0.2609	185.85

Table 6 (concluded):

BULK PROPERTIES OF Al-Ni-Cu-Au ALLOYS						
Conf.	ΔH_{rigid}	$\Delta H_{relaxed}$	E_c	a	l	B
(-6,-12,6,12)						
186	-0.16024	-0.33276	4.3502	3.7353	0.2608	185.90
187	-0.16068	-0.33302	4.3505	3.7352	0.2608	185.89
188	-0.16251	-0.33451	4.3520	3.7350	0.2609	185.96
189,190	-0.16842	-0.33910	4.3566	3.7343	0.2608	186.200
(-9,-9,6,12)						
174	0.26635	0.02206	4.0638	3.7688	0.2578	176.18
177	0.21041	-0.01619	4.1021	3.7610	0.2578	178.28
173	0.10913	-0.09162	4.1775	3.7489	0.2577	182.20
176	-0.04777	-0.20820	4.2941	3.7286	0.2576	188.42
175	-0.07265	-0.22842	4.3143	3.7260	0.2576	189.42

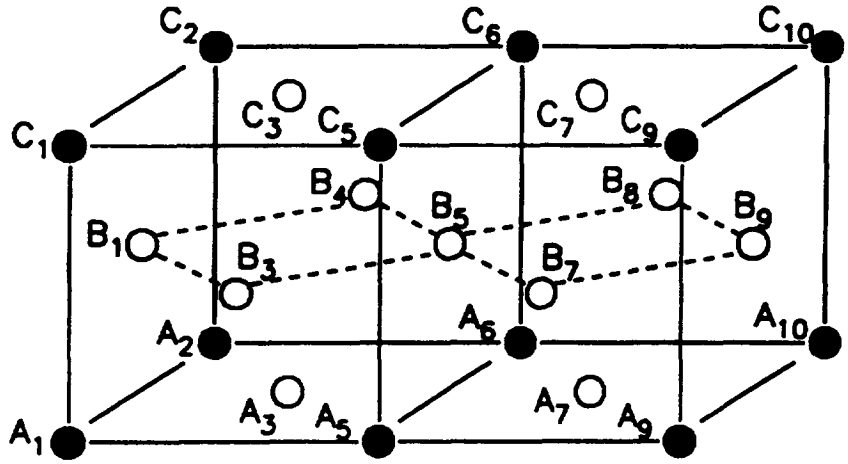

Figure 1: a) A fraction of the calculational cell indicating Ni (circles) and Al atoms (disks) in the Ni_3Al $L1_2$ structure. Each atom is labeled with the plane to which it belongs (A, B, C and D) and a numerical label from 1 to 12, according to the ordering shown in b).

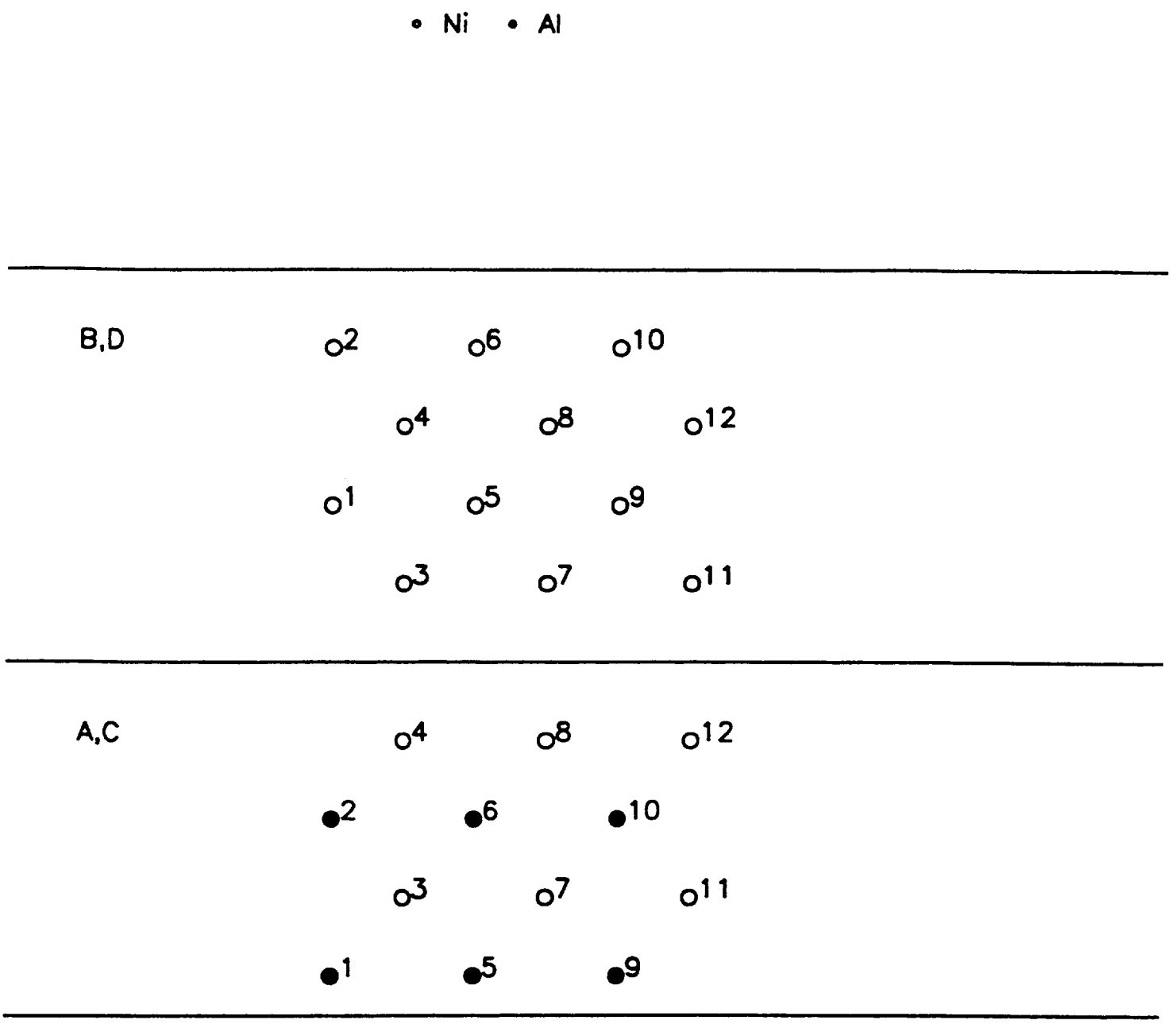
• Ni • Al
B,D
o2 o6 o10
o4 o8 o12
o1 o5 o9
o3 o7 o11
A,C
o4 o8 o12
●2 ●6 ●10
o3 o7 o11
●1 ●5 ●9

Figure 1.b

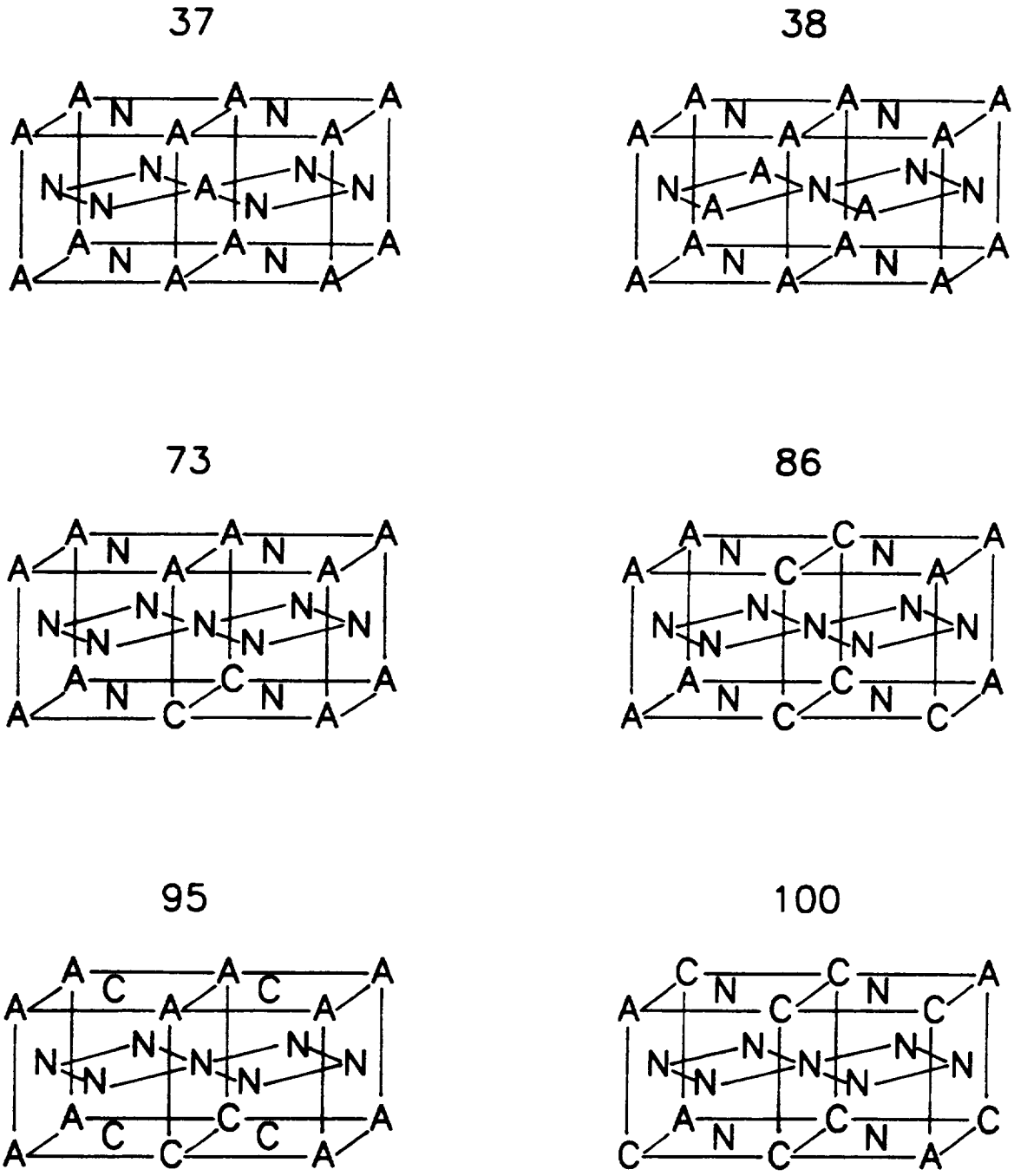

Figure 2: a) Some configurations of interest (see text). Configurations #37 and 38 correspond to binary Al-Ni alloys (N and A indicate Ni and Al atoms respectively). Configurations #73-100 denote some ternary Al-Ni-Cu (C indicates Cu atoms) alloys. b) Ternary and quaternary ordered structures, including Al, Ni, Cu and Au (indicated by the symbol A) atoms.

150

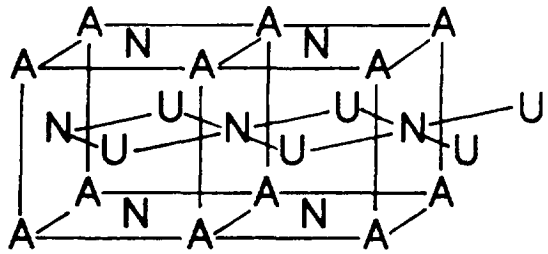

155

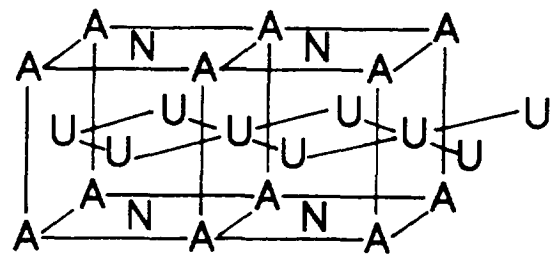

168

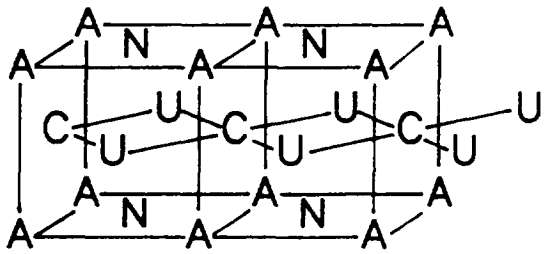

169

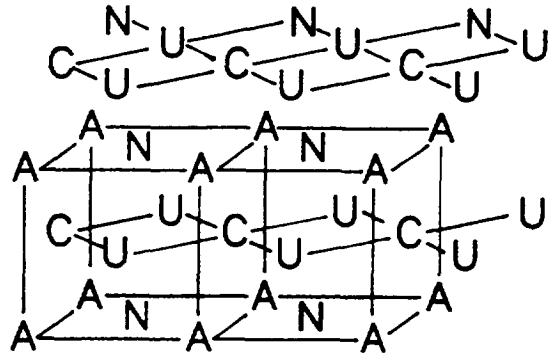

171

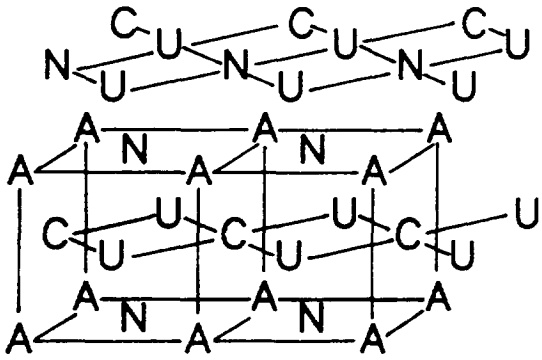

172

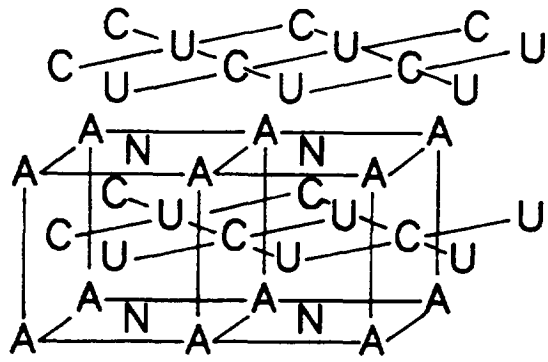

Figure 2.b

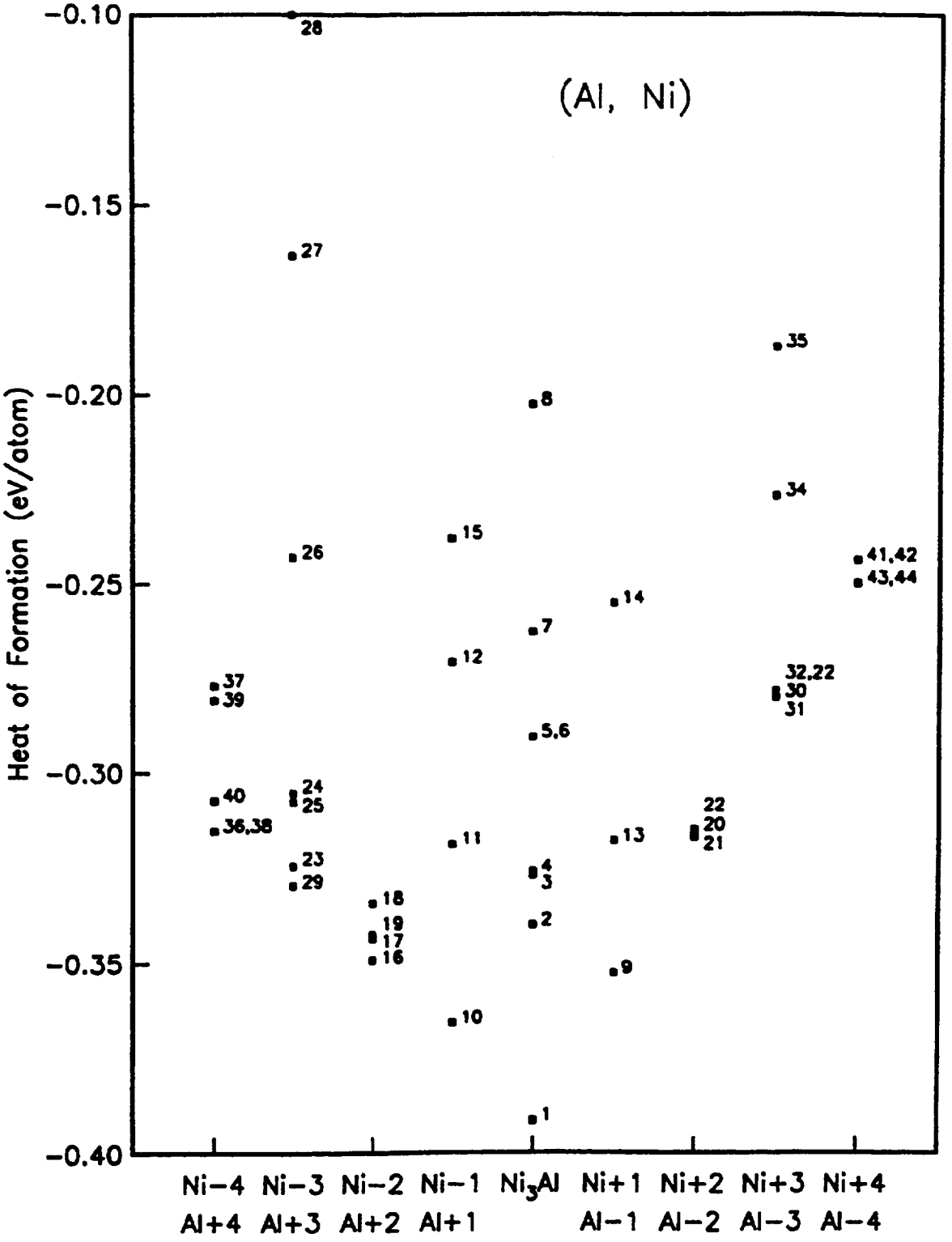

Figure 3: Heat of formation (in eV/atom) for Al-Ni alloys as a function of Ni concentration. The labels correspond to the configurations described in the text (see Appendix). The horizontal axis is labeled according to the number of additional (or missing) Ni and Al atoms with respect to the Ni_3Al alloy.

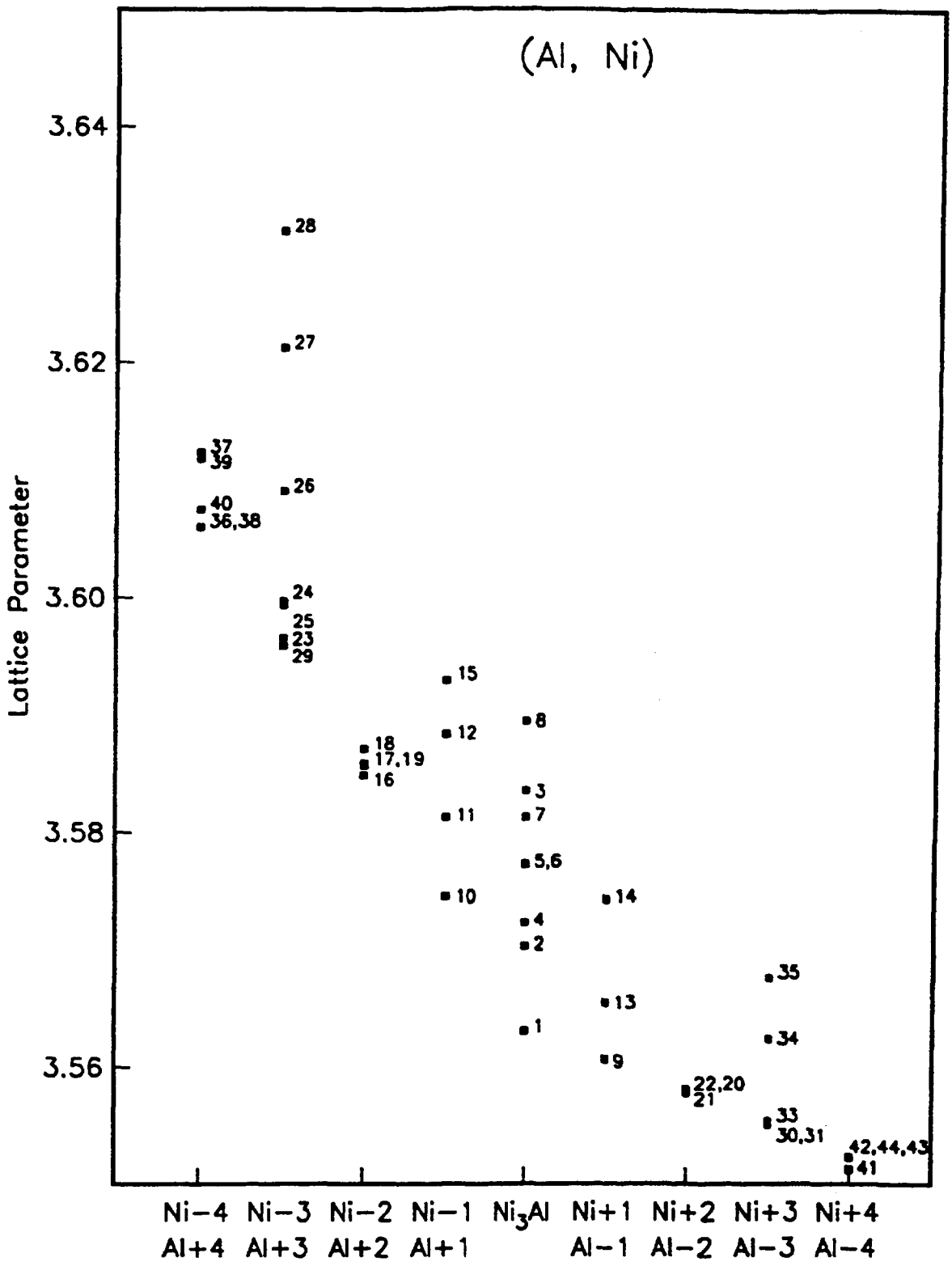

Figure 4: Lattice parameter a (in Å) for the Al-Ni alloys shown in Fig. 3, as a function of Ni concentration.

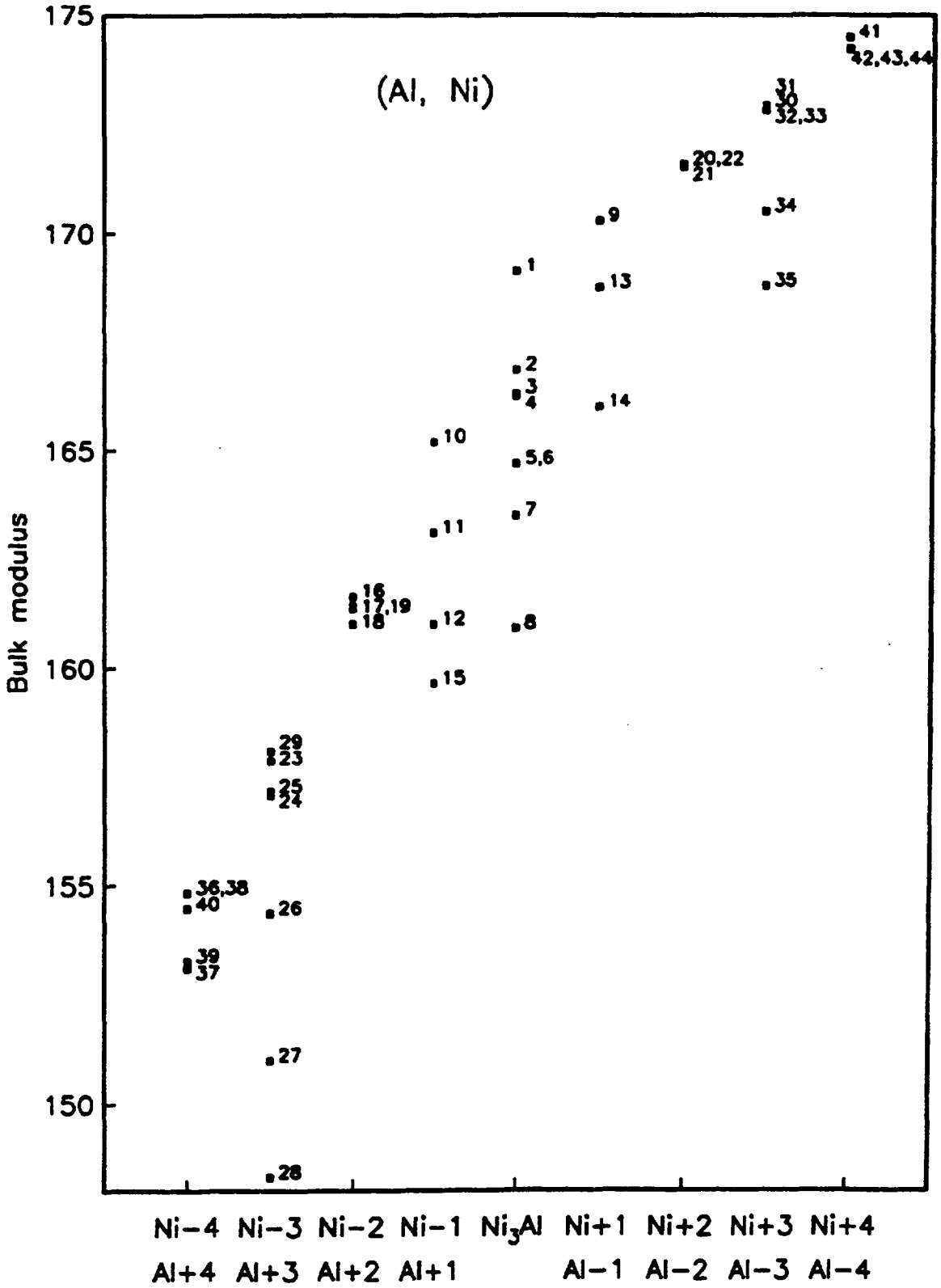

Figure 5: Bulk modulus B (in 10^{10} dynes/cm^2) for Al-Ni alloys as a function of Ni concentration (see Fig. 3).

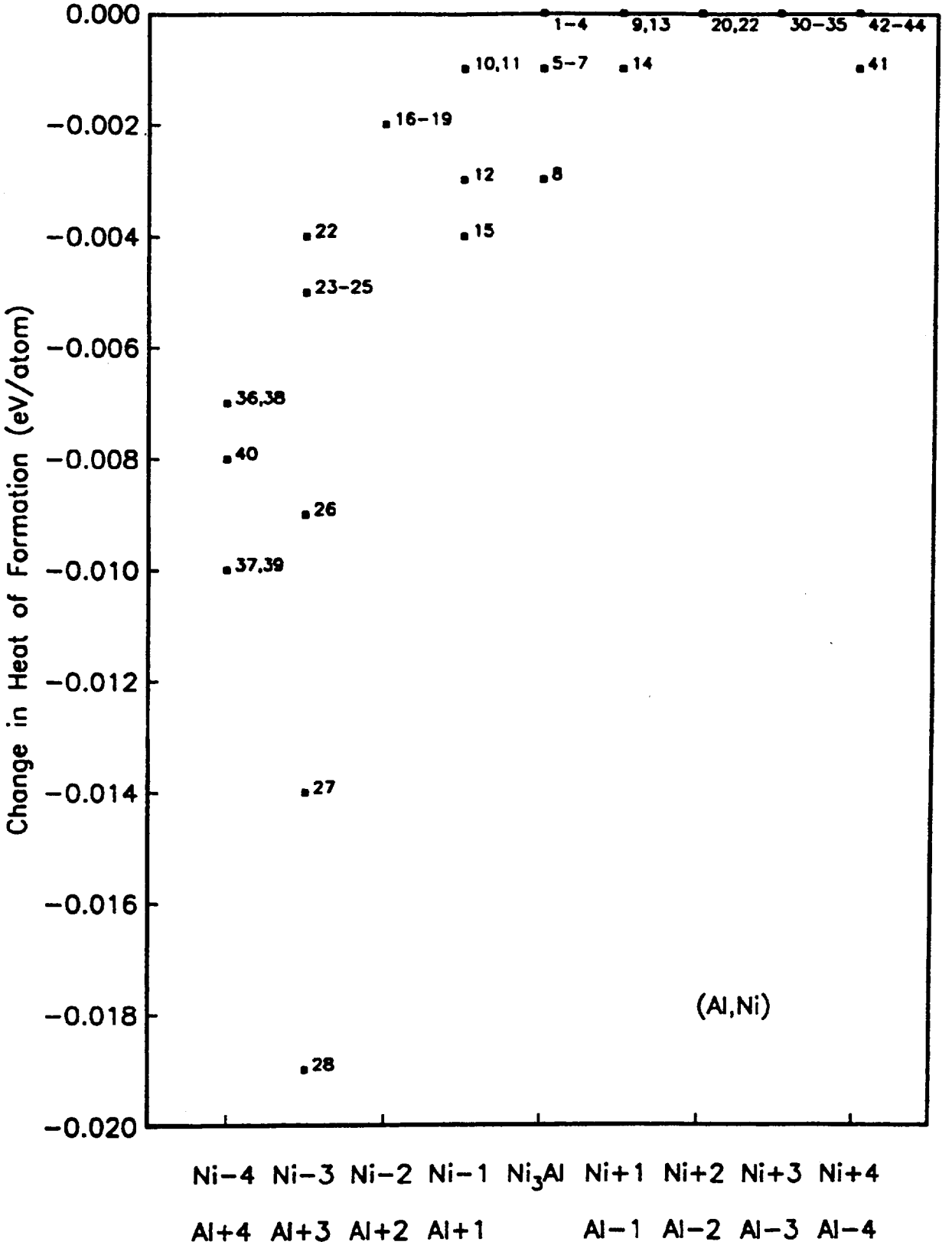

Figure 6: Net change in heat of formation (in eV/atom) between the different Al-Ni alloys with respect to the ground state Ni_3Al structure.

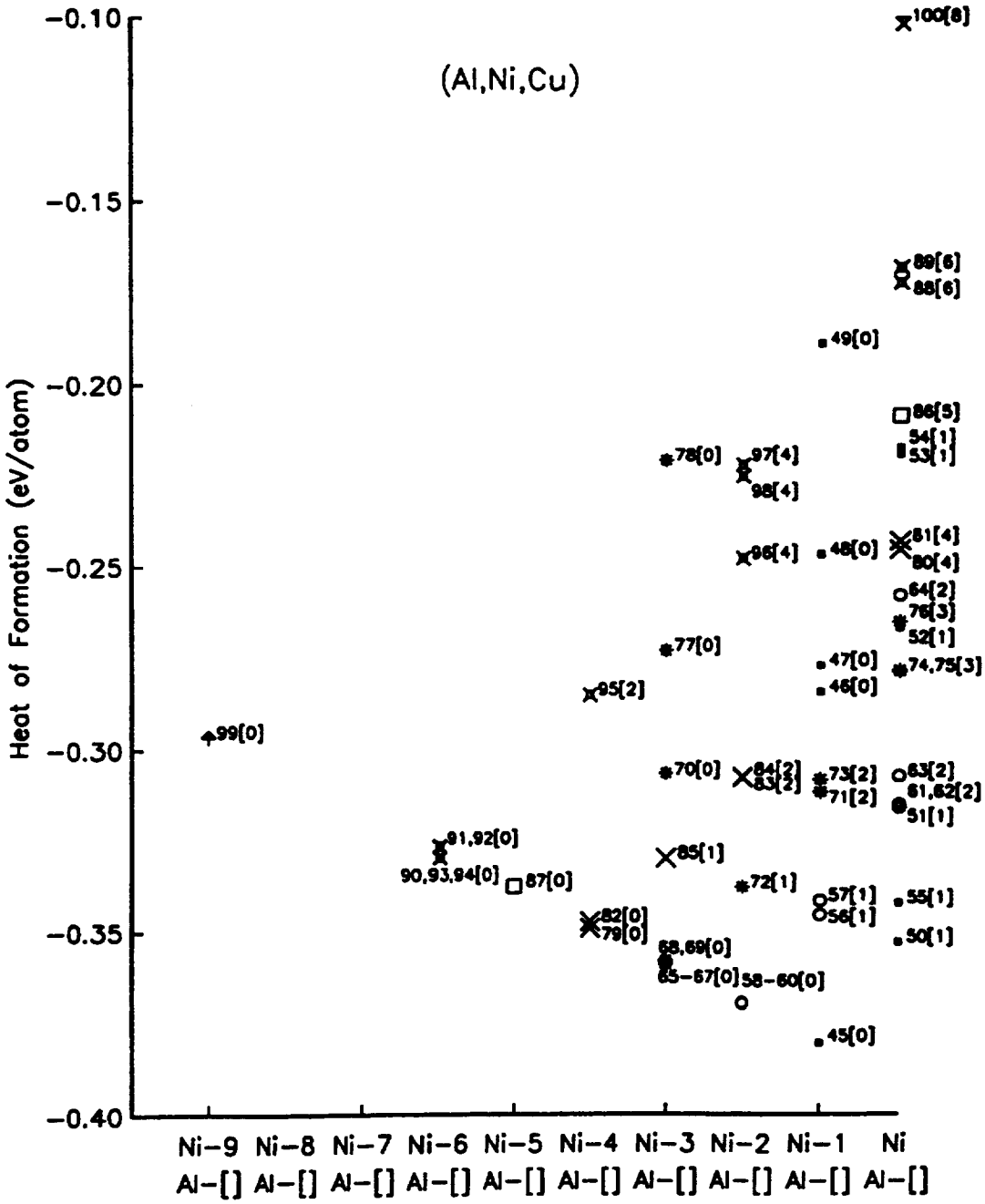

Figure 7: Heat of formation (in eV/atom) of Al-Ni-Cu alloys as a function of Ni concentration. The different symbols correspond to different numbers of Cu impurities in the computational cell: solid squares (one Cu atom), circles (2), asterisks (3), crosses (4), squares (5), slashed square (6), campstool (8) and arrows (9). The number between square brackets indicate the number of Al atoms substituted by impurities. For example, the symbol 95[2] indicates configuration # 95, with 6 Cu impurities in the computational cell, two of them occupying Al sites and four in Ni sites.

58

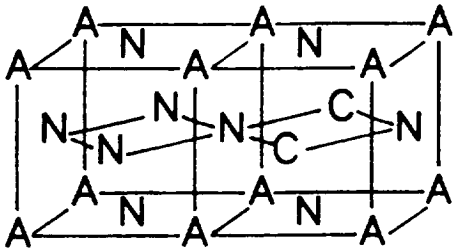

65

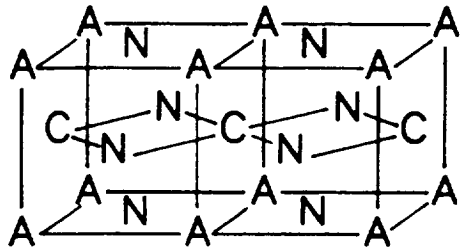

82

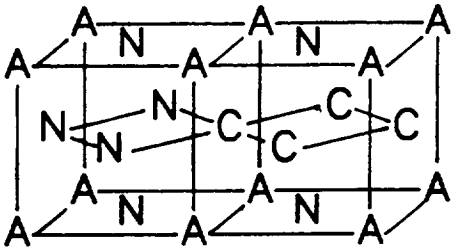

87

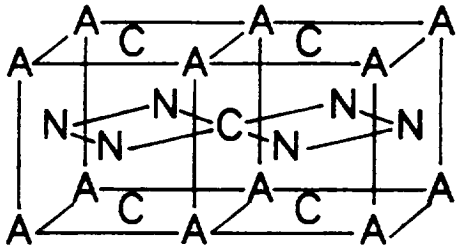

90

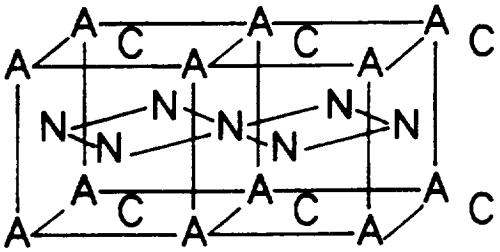

99

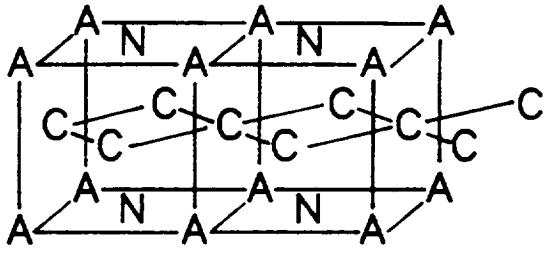

Figure 8: Series of configurations belonging to the boundary line in Fig. 8 (see text).

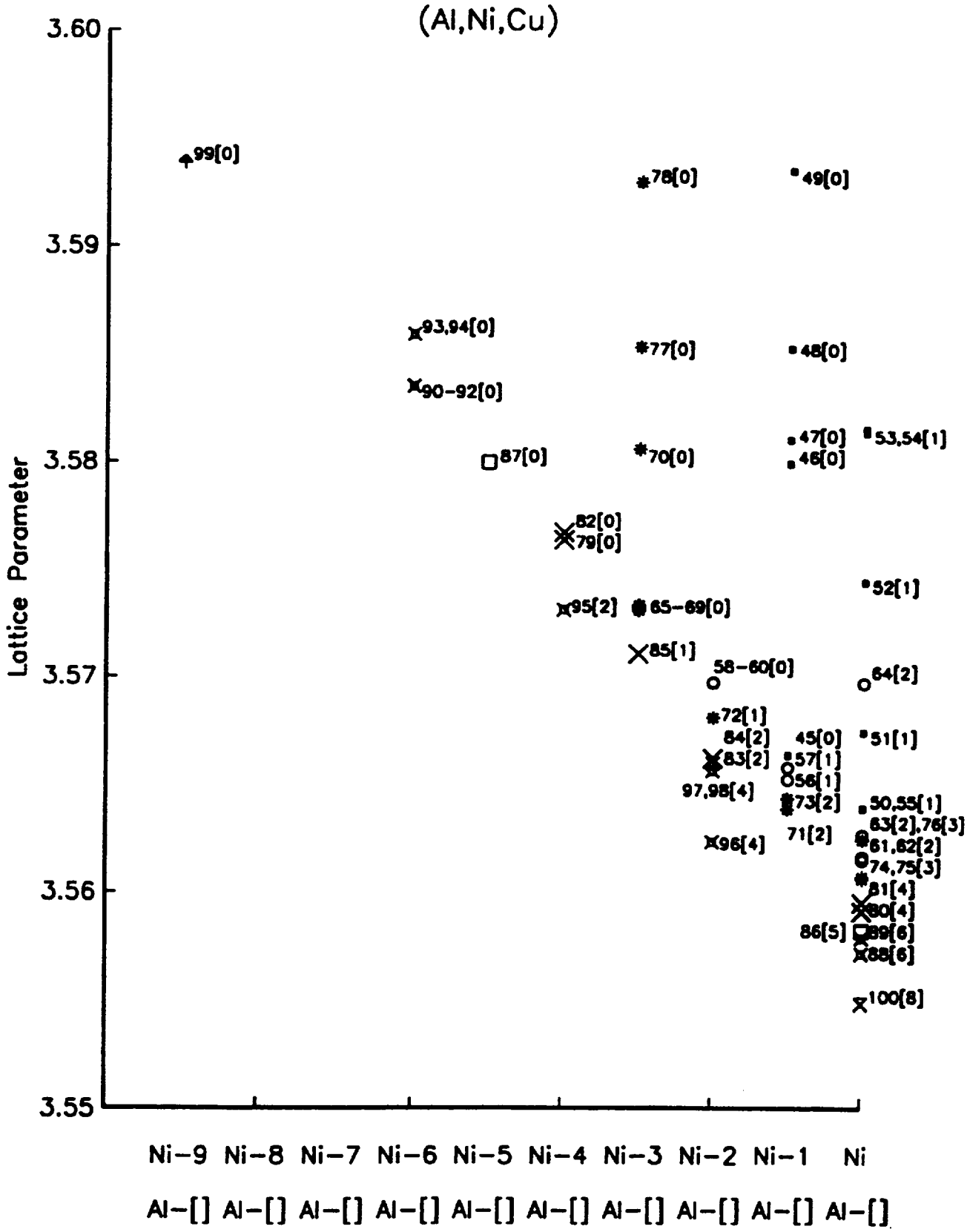

Figure 9: Lattice parameter a (in Å) for Al-Ni-Cu alloys as a function of Ni concentration. See caption for Fig. 7 for explanation of symbols used.

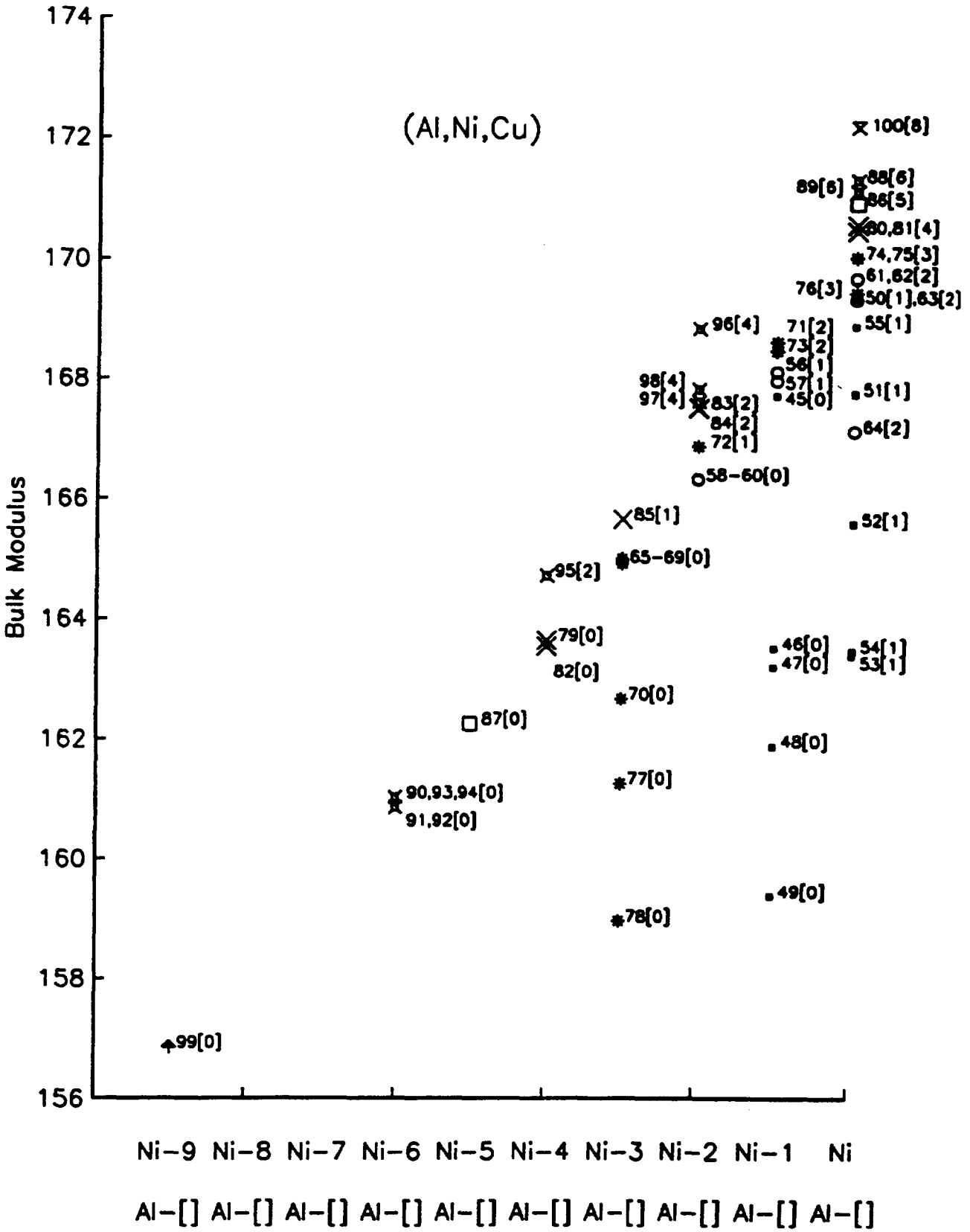

Figure 10: Bulk modulus B for Al-Ni-Cu alloys as a function of Ni concentration. See caption for Fig. 7 for explanation of symbols used.

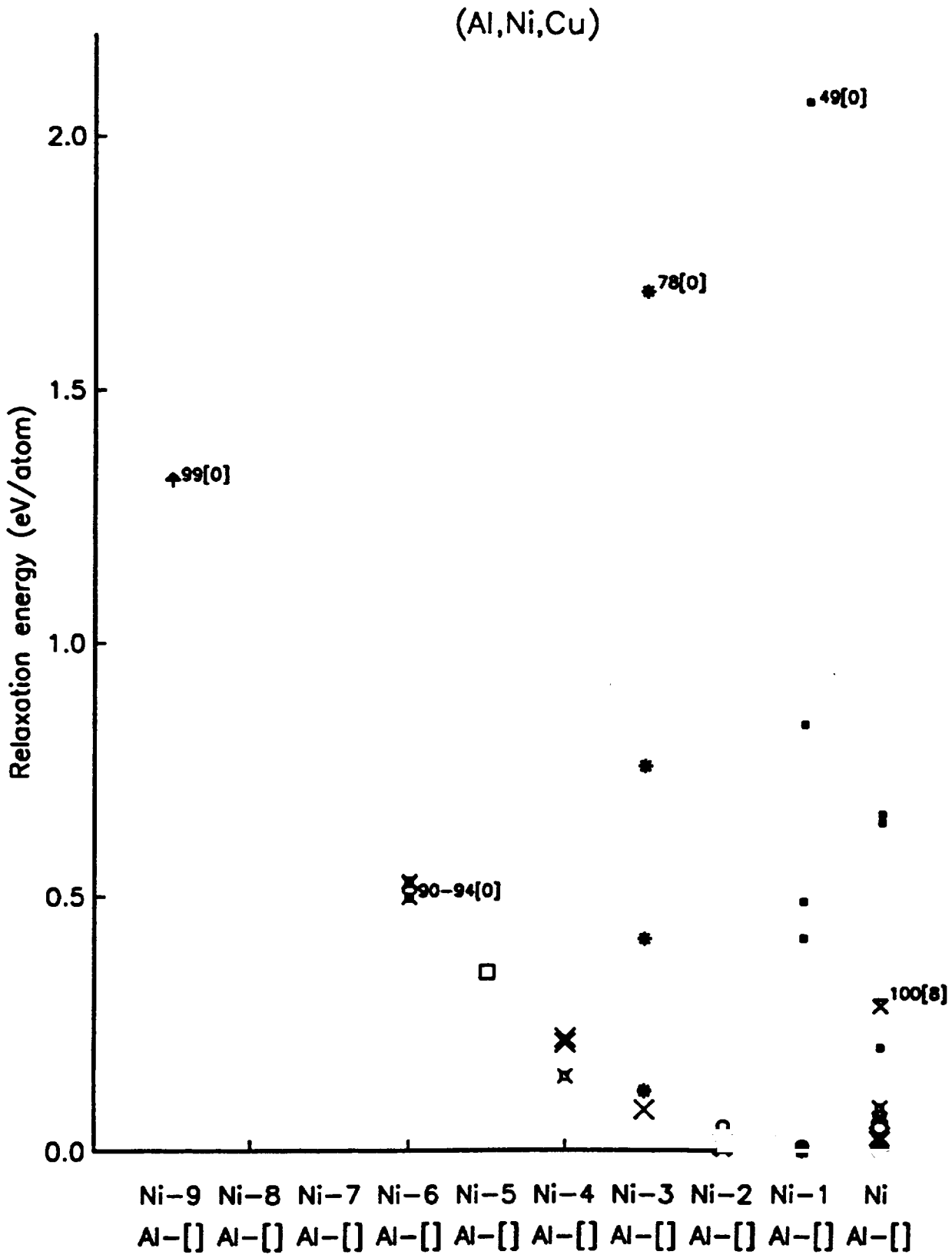

Figure 11: Relaxation energy (in eV/atom) for Al-Ni-Cu alloys (difference in energy of formation between the relaxed alloy and the reference Ni_3Al $L1_2$ ordered alloy. Symbols used are the same as in previous figures.

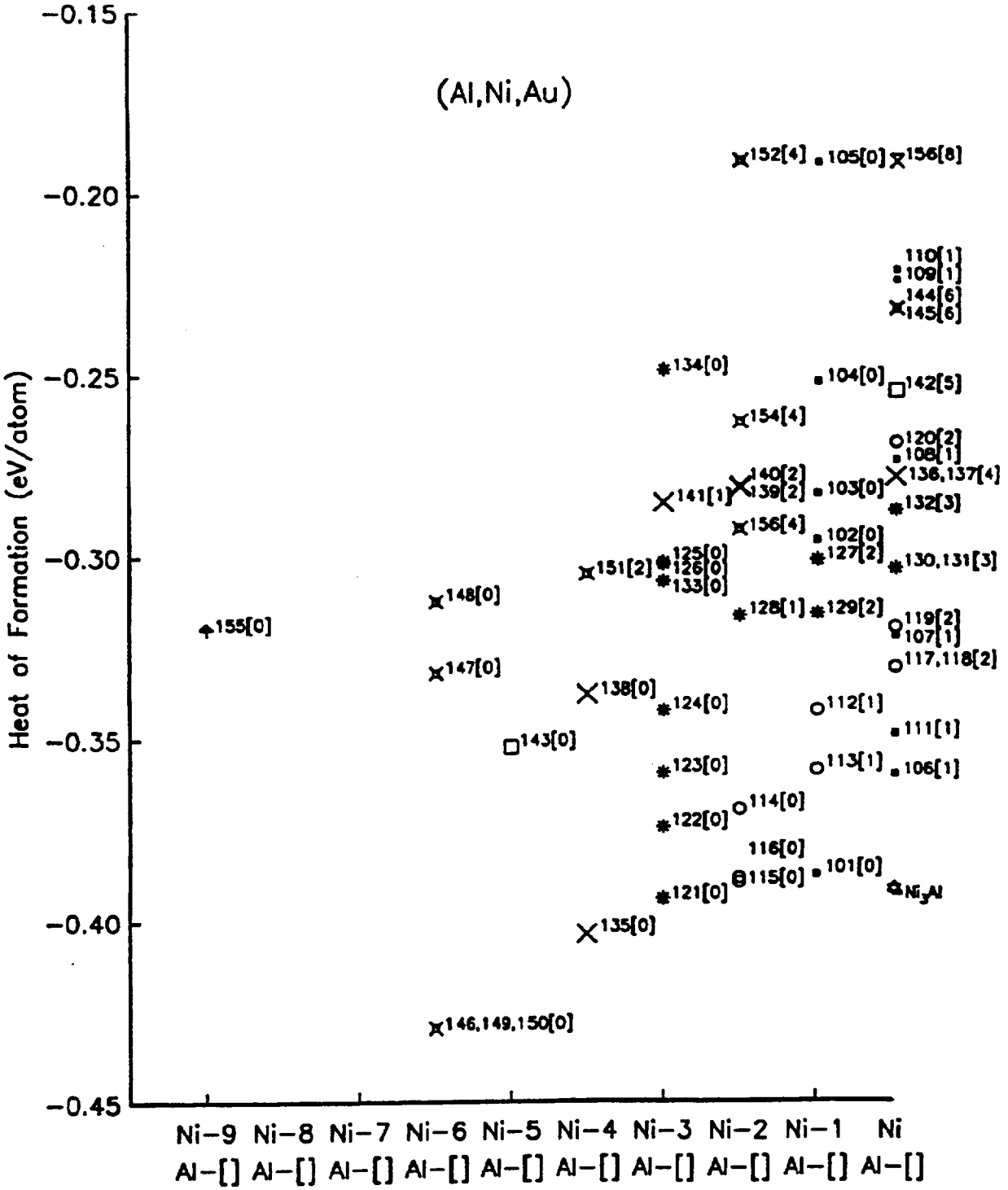

Figure 12: Heat of formation (in eV/atom) of Al-Ni-Au alloys as a function of Ni concentration. The different symbols correspond to different numbers of Au impurities in the computational cell: solid squares (one Au atom), circles (2), asterisks (3), crosses (4), squares (5), slashed square (6), campstool (8) and arrows (9). The number between square brackets indicate the number of Al atoms substituted by impurities (see Fig. 7).

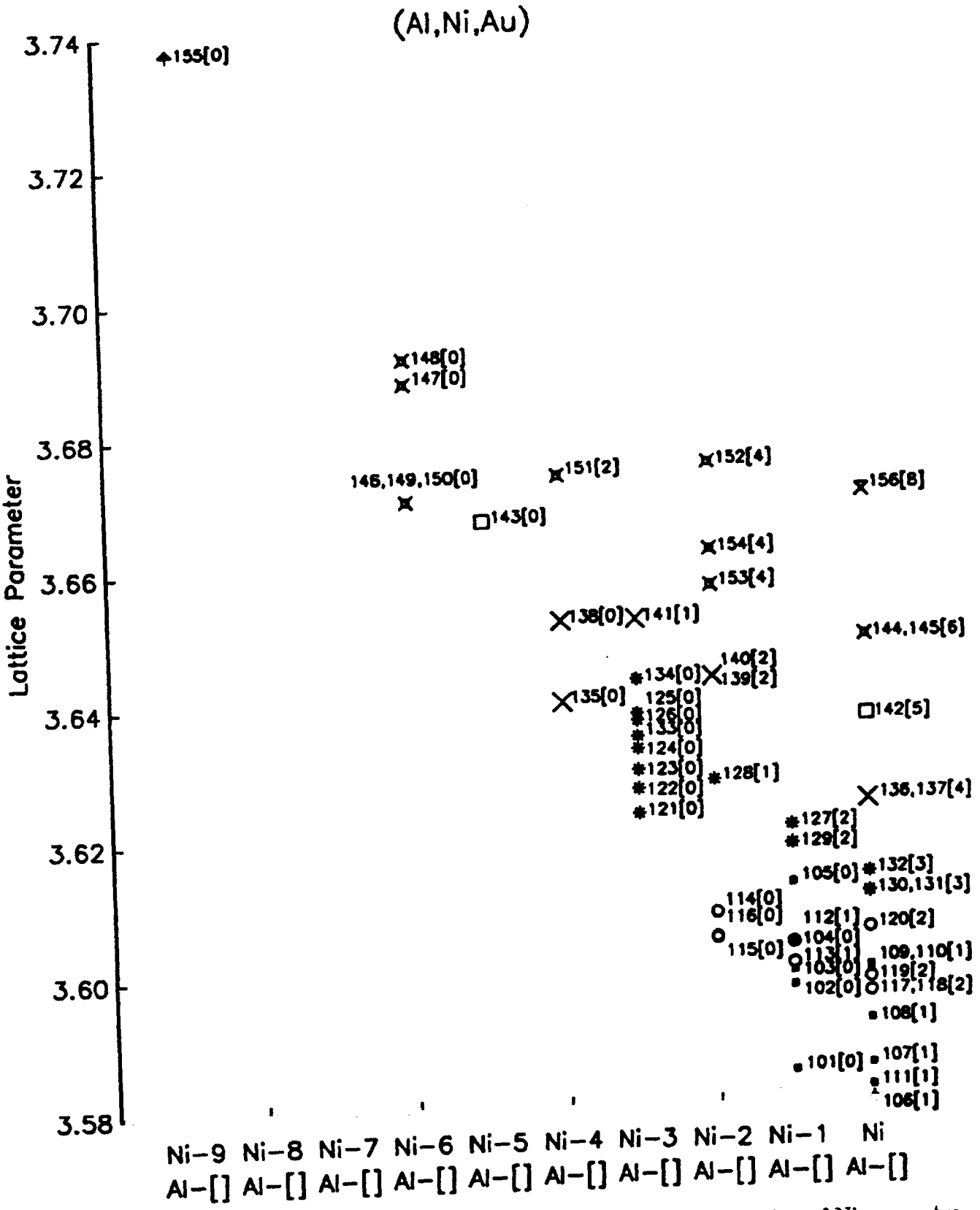

Figure 13: Lattice parameter a (in Å) for Al-Ni-Au alloys as a function of Ni concentration. See caption for Fig. 12 for explanation of symbols used.

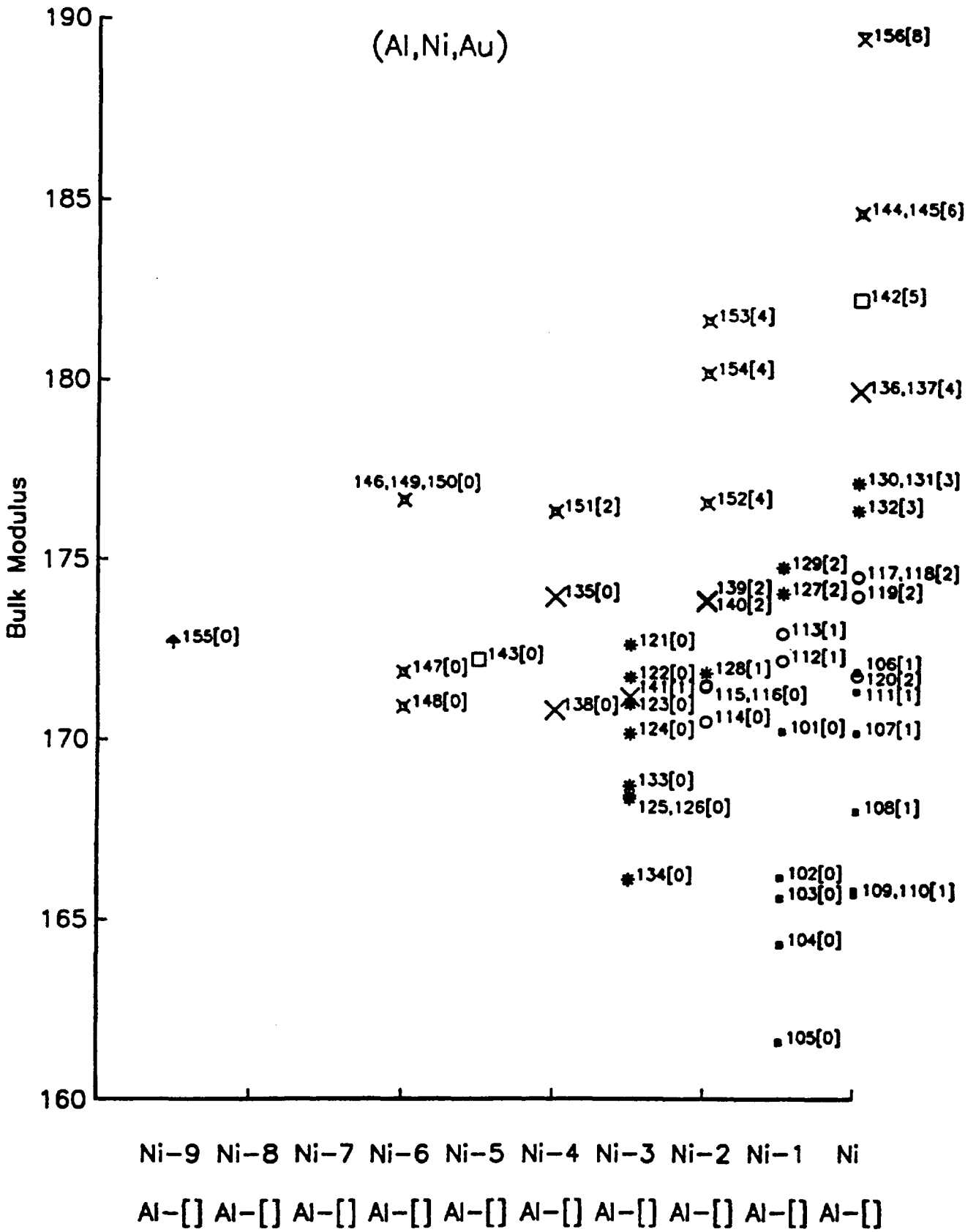

Figure 14: Bulk modulus B for Al-Ni-Au alloys as a function of Ni concentration. See caption for Fig. 12 for explanation of symbols used.

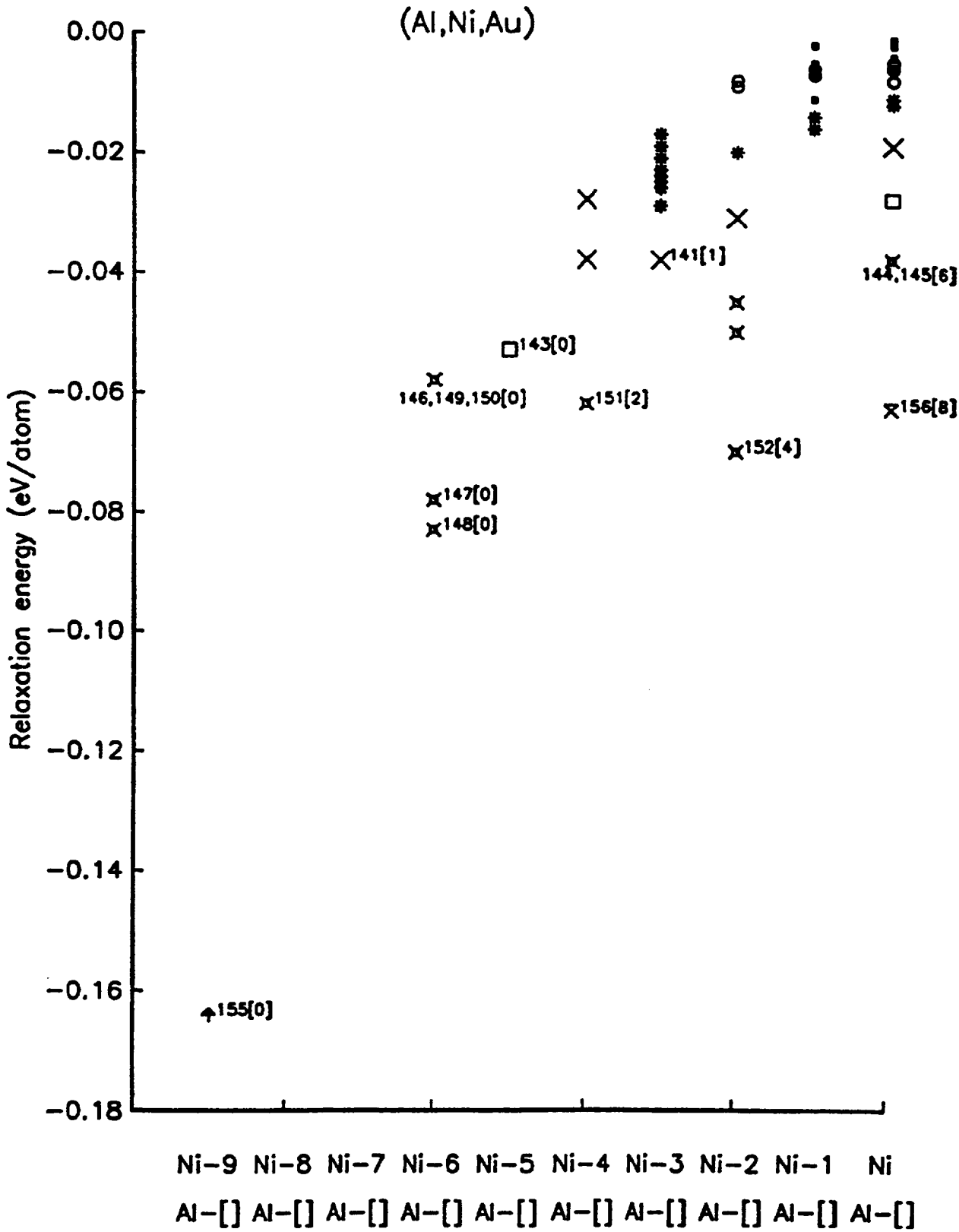

Figure 15: Relaxation energy (in eV/atom) of Al-Ni-Au alloys (difference in energy of formation between the relaxed alloy and the reference Ni_3Al $L1_2$ ordered alloy. Symbols used are the same as in previous figures.

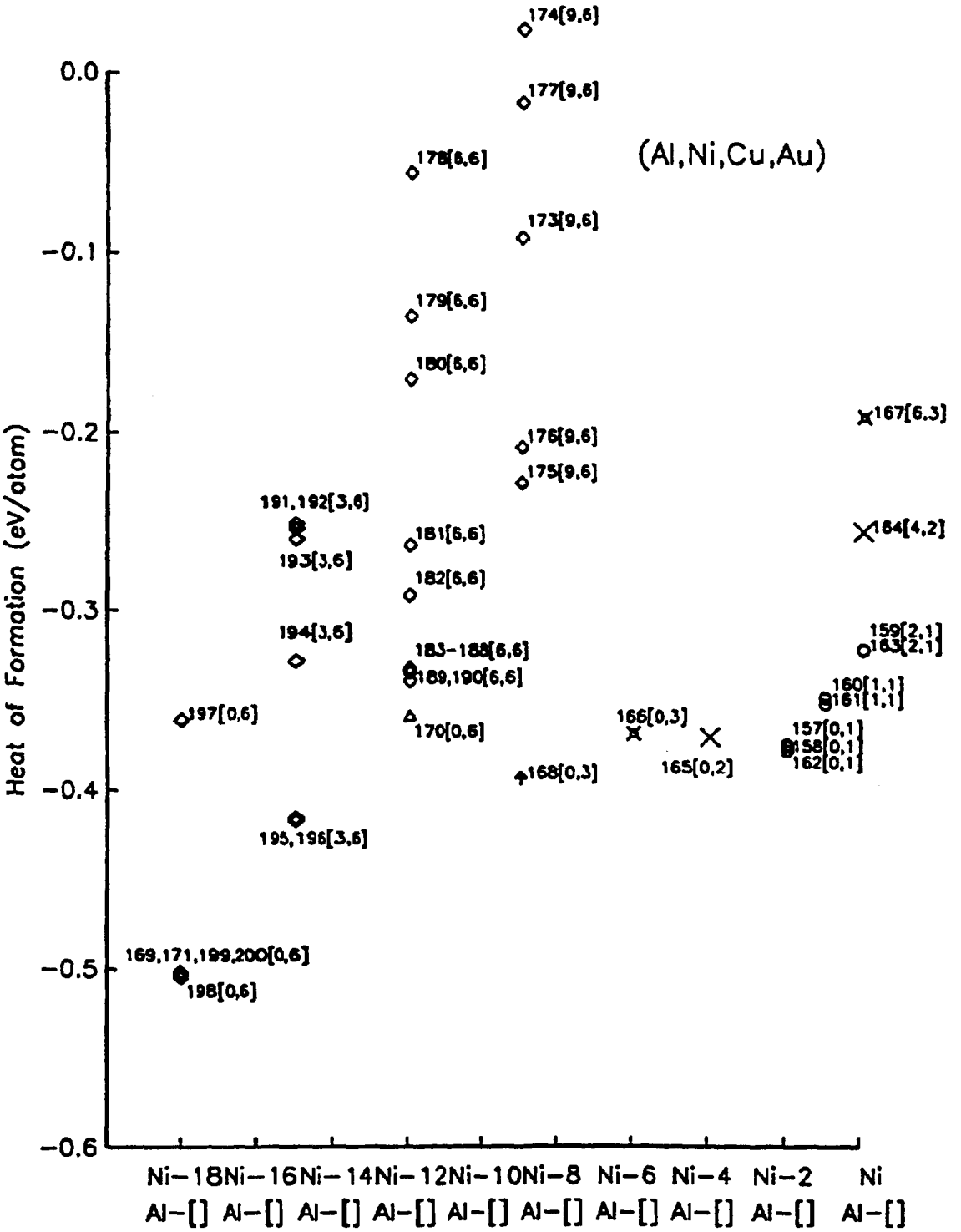

Figure 16: heat of formation (in eV/atom) of Al-Ni-Cu-Au alloys as a function of Ni concentration. The different symbols correspond to different numbers of impurity atoms (Cu, Au or both) (see text) in the computational cell: solid squares (one impurity atom), circles (2), asterisks (3), crosses (4), squares (5), slashed square (6), campstool (8) and arrows (9). The number between square brackets indicate the number of Al atoms substituted by impurities.

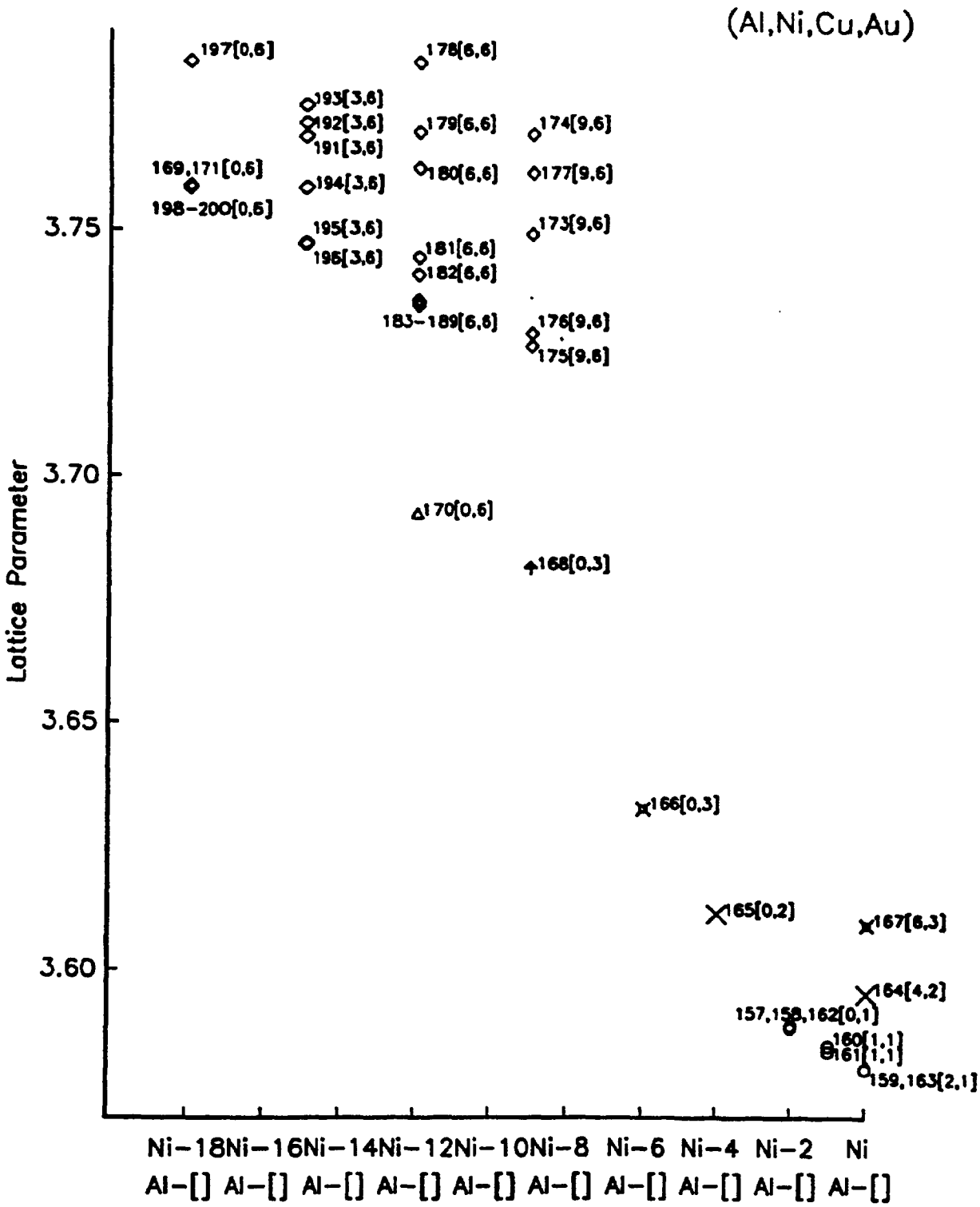

Figure 17: Lattice parameter a (in Å) for Al-Ni-Cu-Au alloys as a function of Ni concentration. See caption for Fig. 16 for explanation of symbols used.

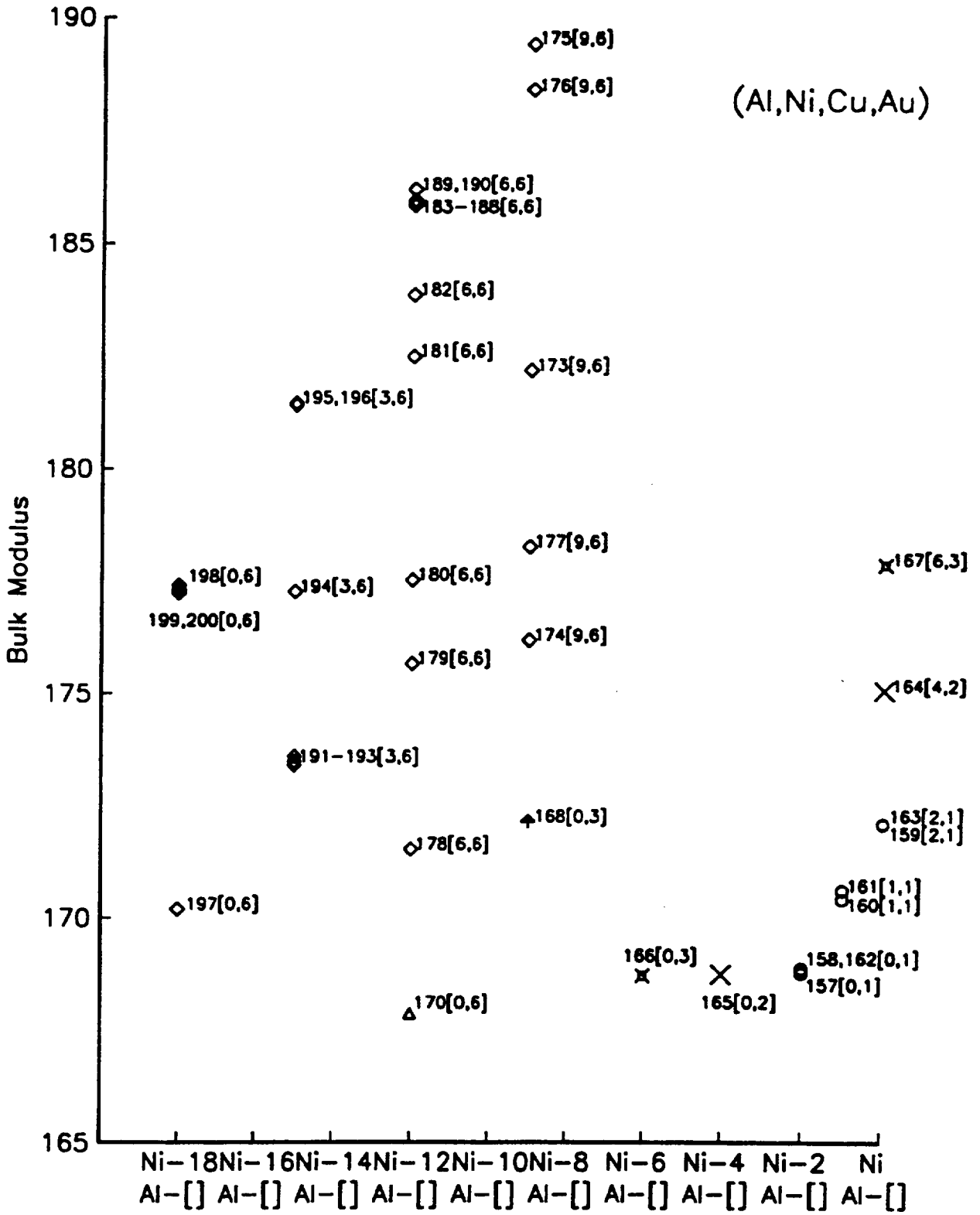

Figure 18: Bulk modulus B for Al-Ni-Cu-Au alloys as a function of Ni concentration. See caption for Fig. 17 for explanation of symbols used.

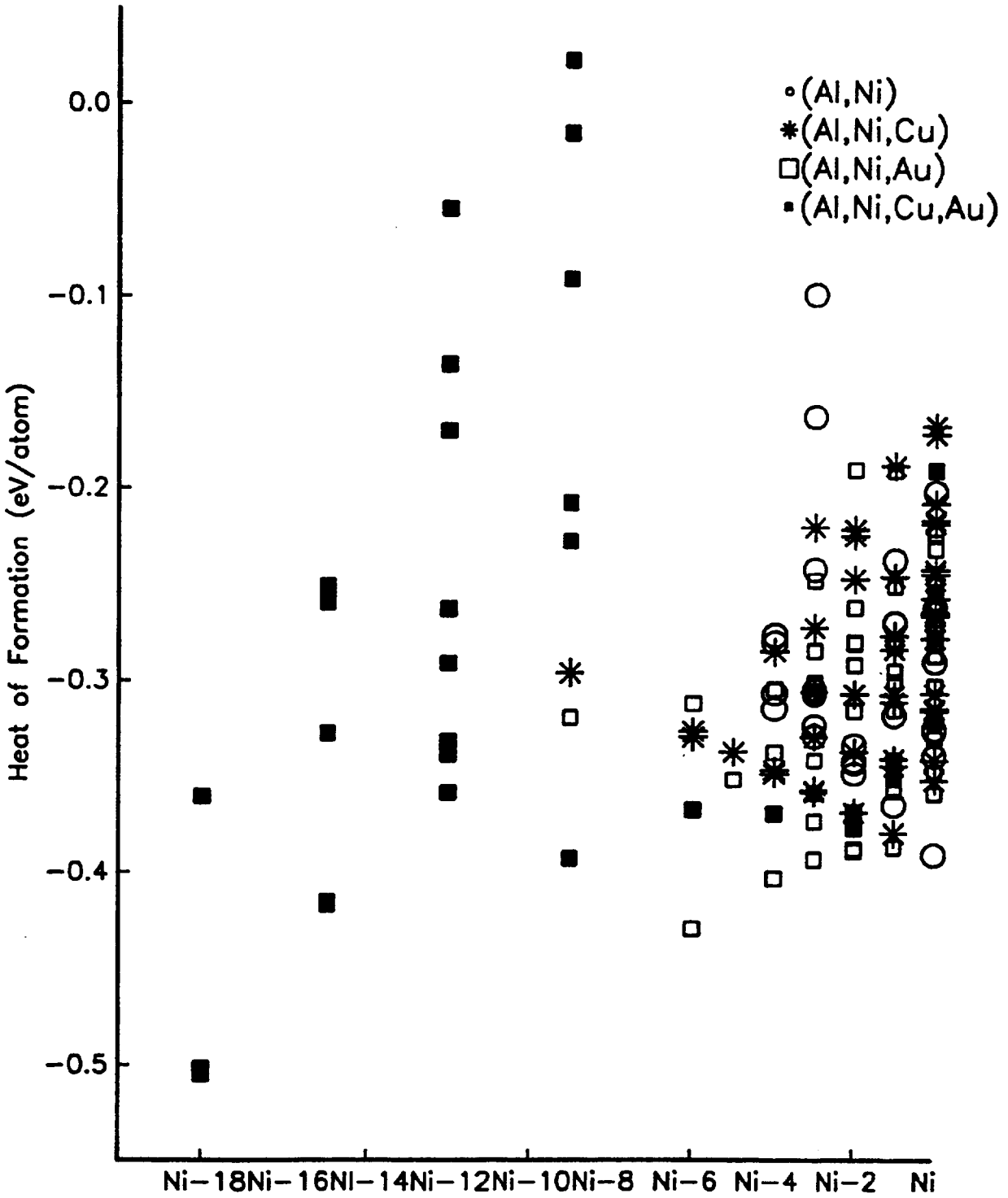

Figure 19: Compilation of the results shown in Figs. 3, 7, 12 and 16 for the heat of formation (in eV/atom) as a function of Ni composition for most of the alloys studied in this work. The different symbols indicate the type of alloys: circles denote Al-Ni alloys, Al-Ni-Cu alloys and Al-Ni-Au are denoted with asterisks and squares respectively. Quaternary Al-Ni-Cu-Au alloys are labeled with solid squares.

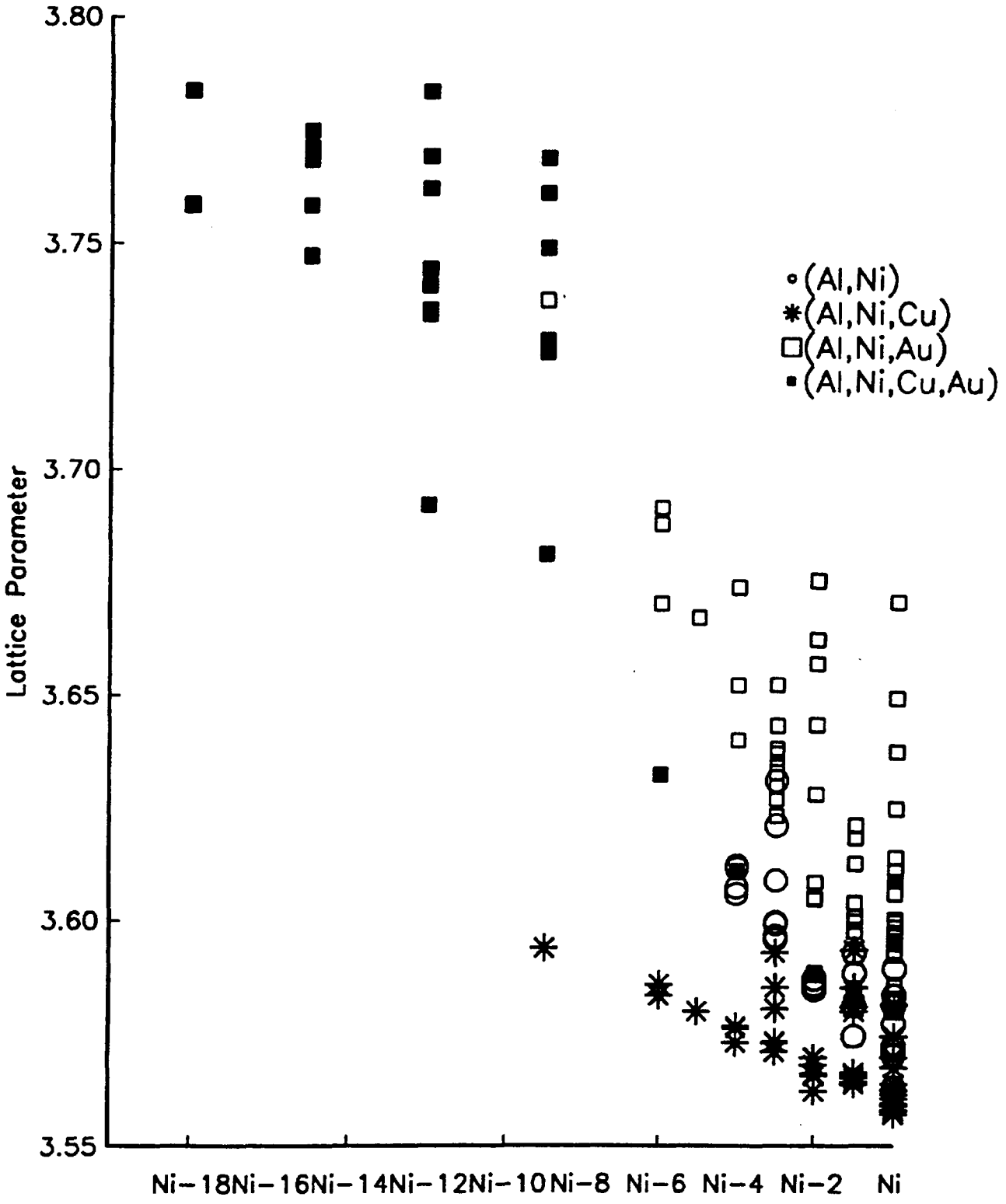

Figure 20: Compilation of the results shown in Figs. 4, 9, 13 and 17 for the lattice parameter a (in Å) as a function of Ni composition for all the alloys studied in this work. The symbols used to indicate the different families of alloys are the same as in Fig. 19.

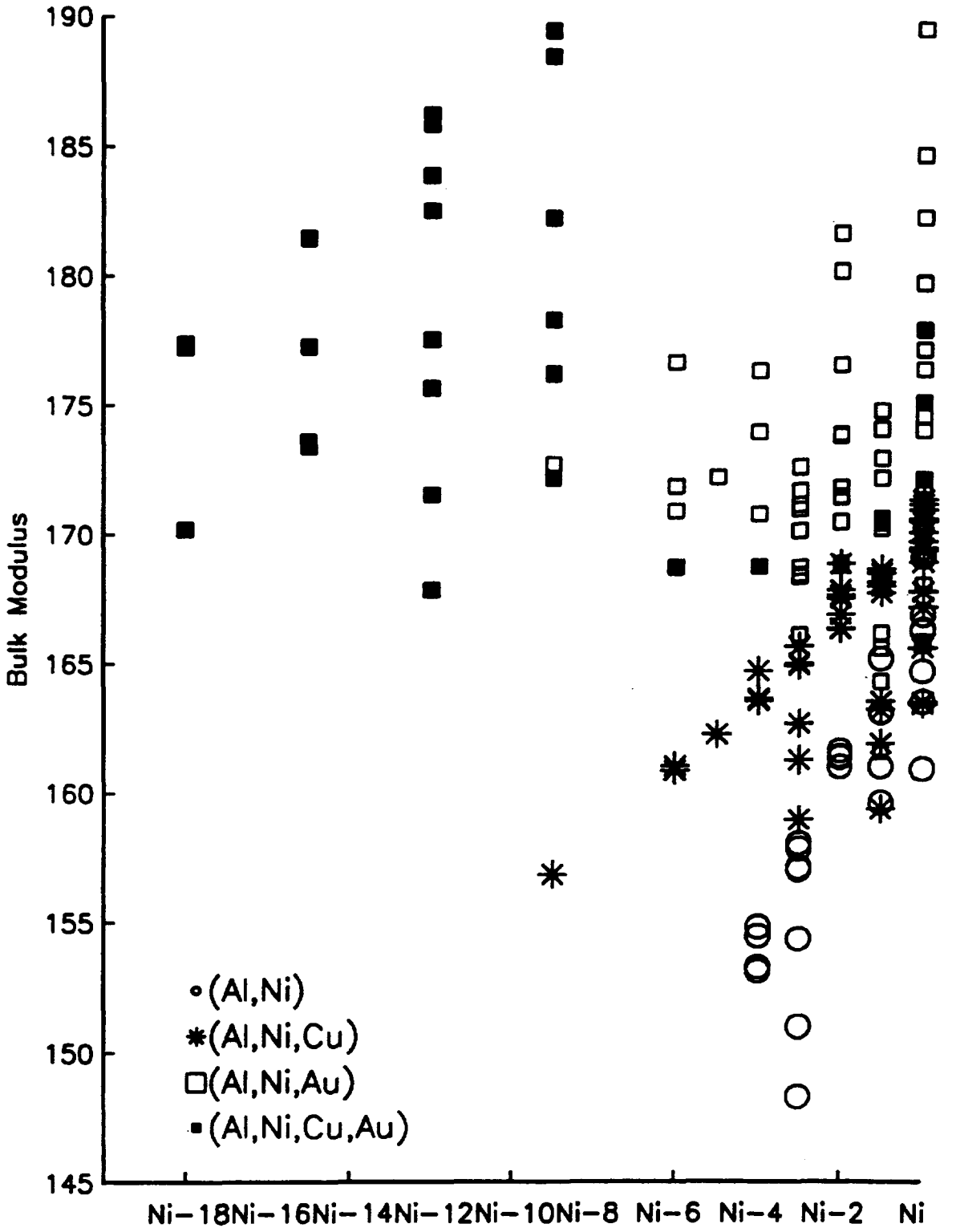

Figure 21: Compilation of the results shown in Figs. 5, 10, 14 and 18 for the bulk modulus B as a function of Ni composition for all the alloys studied in this work.The symbols used to indicate the different families of alloys are the same as in Fig. 19.

REPORT DOCUMENTATION PAGE

Form Approved
OMB No. 0704-0188

1. AGENCY USE ONLY (*Leave blank*)	2. REPORT DATE	3. REPORT TYPE AND DATES COVERED
	April 1995	Technical Memorandum

4. TITLE AND SUBTITLE

Bulk Properties of $Ni_3Al(\gamma')$ With Cu and Au Additions

5. FUNDING NUMBERS

WU-505-90-53

6. AUTHOR(S)

Guillermo Bozzolo and John Ferrante

7. PERFORMING ORGANIZATION NAME(S) AND ADDRESS(ES)

National Aeronautics and Space Administration
Lewis Research Center
Cleveland, Ohio 44135-3191

8. PERFORMING ORGANIZATION REPORT NUMBER

E-9602

9. SPONSORING/MONITORING AGENCY NAME(S) AND ADDRESS(ES)

National Aeronautics and Space Administration
Washington, D.C. 20546-0001

10. SPONSORING/MONITORING AGENCY REPORT NUMBER

NASA TM-106905

11. SUPPLEMENTARY NOTES

Guillermo Bozzolo, Analex Corporation, 3001 Aerospace Parkway, Brook Park, Ohio 44142 (work funded by NASA Contract NAS3-25776); John Ferrante, NASA Lewis Research Center. Responsible person, John Ferrante, organization code 0130, (216) 433-6069.

12a. DISTRIBUTION/AVAILABILITY STATEMENT

Unclassified - Unlimited
Subject Category 26

This publication is available from the NASA Center for Aerospace Information, (301) 621-0390.

12b. DISTRIBUTION CODE

13. ABSTRACT ***(Maximum 200 words)***

The BFS method for alloys is applied to the study of 200 alloys obtained from adding Cu and Au impurities to a Ni_3Al matrix. We analyze the trends in the bulk properties of these alloys (heat of formation, lattice parameter and bulk modulus) and detect specific alloy compositions for which these quantities have particular values. A detailed analysis of the atomic interactions that lead to the preferred ordering patterns is presented.

14. SUBJECT TERMS

Keyboards; Alloys; Nickel; Aluminum

15. NUMBER OF PAGES

74

16. PRICE CODE

A04

17. SECURITY CLASSIFICATION OF REPORT	18. SECURITY CLASSIFICATION OF THIS PAGE	19. SECURITY CLASSIFICATION OF ABSTRACT	20. LIMITATION OF ABSTRACT
Unclassified	Unclassified	Unclassified	

National Aeronautics and
Space Administration

Lewis Research Center
21000 Brookpark Rd.
Cleveland, OH 44135-3191